

## Article (refereed) - postprint

Boyer, Patrick; Wells, Claire; Howard, Brenda. 2018. **Extended Kd distributions for freshwater environment.** *Journal of Environmental Radioactivity*, 192. 128-142. <https://doi.org/10.1016/j.jenvrad.2018.06.006>

© 2018 Elsevier Ltd.

This manuscript version is made available under the CC-BY-NC-ND 4.0 license <http://creativecommons.org/licenses/by-nc-nd/4.0/>



This version available <http://nora.nerc.ac.uk/id/eprint/520590/>

NERC has developed NORA to enable users to access research outputs wholly or partially funded by NERC. Copyright and other rights for material on this site are retained by the rights owners. Users should read the terms and conditions of use of this material at <http://nora.nerc.ac.uk/policies.html#access>

NOTICE: this is the author's version of a work that was accepted for publication in *Journal of Environmental Radioactivity*. Changes resulting from the publishing process, such as peer review, editing, corrections, structural formatting, and other quality control mechanisms may not be reflected in this document. Changes may have been made to this work since it was submitted for publication. A definitive version was subsequently published in *Journal of Environmental Radioactivity*, 192. 128-142. <https://doi.org/10.1016/j.jenvrad.2018.06.006>

[www.elsevier.com/](http://www.elsevier.com/)

Contact CEH NORA team at  
[noraceh@ceh.ac.uk](mailto:noraceh@ceh.ac.uk)

The NERC and CEH trademarks and logos ('the Trademarks') are registered trademarks of NERC in the UK and other countries, and may not be used without the prior written consent of the Trademark owner.

## Article (refereed) - postprint

Boyer, Patrick; Wells, Claire; Howard, Brenda. 2018. **Extended Kd distributions for freshwater environment.** *Journal of Environmental Radioactivity*, 192. 128-142. <https://doi.org/10.1016/j.jenvrad.2018.06.006>

© 2018 Elsevier B.V.

This manuscript version is made available under the CC-BY-NC-ND 4.0 license <http://creativecommons.org/licenses/by-nc-nd/4.0/>



This version available <http://nora.nerc.ac.uk/id/eprint/520590/>

NERC has developed NORA to enable users to access research outputs wholly or partially funded by NERC. Copyright and other rights for material on this site are retained by the rights owners. Users should read the terms and conditions of use of this material at <http://nora.nerc.ac.uk/policies.html#access>

NOTICE: this is the author's version of a work that was accepted for publication in *Journal of Environmental Radioactivity*. Changes resulting from the publishing process, such as peer review, editing, corrections, structural formatting, and other quality control mechanisms may not be reflected in this document. Changes may have been made to this work since it was submitted for publication. A definitive version was subsequently published in *Journal of Environmental Radioactivity*, 192. 128-142. <https://doi.org/10.1016/j.jenvrad.2018.06.006>

[www.elsevier.com/](http://www.elsevier.com/)

Contact CEH NORA team at  
[noraceh@ceh.ac.uk](mailto:noraceh@ceh.ac.uk)

The NERC and CEH trademarks and logos ('the Trademarks') are registered trademarks of NERC in the UK and other countries, and may not be used without the prior written consent of the Trademark owner.

*Extended  $K_d$  distributions for freshwater environment*

Boyer P.<sup>(a)</sup>, Wells C.<sup>(b)</sup>, Howard B.<sup>(b)</sup>

<sup>(a)</sup> Institut de Radioprotection et de Sûreté Nucléaire (IRSN), PSE-ENV, SERTE, LRTA, Cadarache, France

<sup>(b)</sup> Centre for Ecology & Hydrology (CEH), Lancaster, United Kingdom

## **Highlights**

- Solid-liquid fractionation of radionuclides in freshwater environments.
- Update of the freshwater  $K_d$  databases for 49 chemical elements.
- Log-normal distributions of  $K_d$  values
- Mass/Volume ratio effect on  $K_d$  distributions of suspended sediments in the field.

## ABSTRACT

Many of the freshwater  $K_d$  values required for quantifying radionuclide transfer in the environment (e.g. ERICA Tool, Symbiose modelling platform) are either poorly reported in the literature or not available. To partially address this deficiency, Working Group 4 of the IAEA program MODARIA (2012-2015) has completed an update of the freshwater  $K_d$  databases and  $K_d$  distributions given in TRS 472 (IAEA, 2010). Over 2300 new values for 27 new elements were added to the dataset and 270 new  $K_d$  values were added for the 25 elements already included in TRS 472 (IAEA, 2010). For 49 chemical elements, the  $K_d$  values have been classified according to three solid-liquid exchange conditions (adsorption, desorption and field) as was previously carried out in TRS 472. Additionally, the  $K_d$  values were classified into two environmental components (suspended and deposited sediments). Each combination (radionuclide x component x condition) was associated with log-normal distributions when there was at least ten  $K_d$  values in the dataset and to a geometric mean when there was less than ten values. The enhanced  $K_d$  dataset shows that  $K_d$  values for suspended sediments are significantly higher than for deposited sediments and that the variability of  $K_d$  distributions are higher for deposited than for suspended sediments. For suspended sediments in field conditions, the variability of  $K_d$  distributions can be significantly reduced as a function of the suspended load that explains more than 50% of the variability of the  $K_d$  datasets of U, Si, Mo, Pb, S, Se, Cd, Ca, B, K, Ra and Po. The distinction between adsorption and desorption conditions is justified for deterministic calculations because the geometric means are systematically greater in desorption conditions. Conversely, this distinction is less relevant for probabilistic calculations due to systematic overlapping between the  $K_d$  distributions of these two conditions.

## 1. INTRODUCTION

IAEA launched several programs, BIOMOV (BIOMOVs, 1990), VAMP (IAEA, 2000), EMRAS I and II (IAEA, 2012), to improve capabilities of the modelling of environmental radiation dose. Those programs aimed (i) to review, improve and update model parameters such as concentration ratios between soil and crops or feed and animal products, and solid/liquid ratios, (ii) model testing, and (iii) comparison of different models and parameter values. In the subsequent IAEA MODARIA program (Modelling and Data for Radiological Impact Assessments, <http://www-ns.iaea.org/projects/modaria/>), Working Group 4 (WG4) aimed to analyse the radioecological data in IAEA Technical Reports Series publications (TRS) to identify key radionuclides and associated parameter values for human and wildlife assessment.

This paper presents recent progress of the IAEA MODARIA WG4 in updating the freshwater  $K_d$  dataset. The improved dataset can be used to derive statistical distributions of freshwater  $K_d$  values which can be applied to assess solid/liquid fractionation of chemical elements associated with radionuclides released or observed in freshwater environments. In these environments, the solid/liquid fractionation of elements is a key process as it directly affects the bioavailability of elements via their transfer pathways. It depends on numerous interactions specific to elements (including radionuclides), properties of solid particles (eg. size, nature, origin) and geochemical conditions (eg. pH, temperature, conductivity) (Sigg et al., 2000; Eguchi, 2017). These conditions influence the complexation (Xu et al., 2014) and oxidation state (Sparks, 2003; Kaplan, 2016) of elements and, consequently, control different mechanisms of solid/liquid partitioning such as dissolution and precipitation (Sposito, 2008), adsorption/desorption (Francis and Brinkley, 1976; Tesoriero and Pankow 1996; Morse et al., 1993; Rivera et al., 2011) and ion exchange (Kabata-Pendias, 2010).

Several approaches exist to model element fractionation such as the Langmuir or Freundlich sorption isotherms (Sparks, 2003), parametric models (Sheppard, 2011; Sheppard et al., 2009), dynamic modelling (Garcia-Sanchez et al., 2014) and mass-action based on thermodynamic models (Goldberg et al., 2007). These different approaches require measuring or assessing a number of environmental variables. However, the lack of relevant and site-specific data for these variables limits the effectiveness of their application in operational models. Consequently, the  $K_d$  approach remains widely used because of its apparent simplicity, its wide availability and the ease of its measurement.

The  $K_d$  is defined as the equilibrium ratio between the mass density of an element sorbed on a solid phase  $C_{solid}$  (mol/kg) and its mass density in the liquid phase  $C_{liquid}$  (mol/L):

$$K_d = \frac{C_{solid}}{C_{liquid}} \text{ (L/kg)} \quad \text{Equation 1}$$

This approach assumes that the adsorption and desorption processes are completely reversible, instantaneously equilibrated and independent of element concentration in the aqueous phase (Sposito, 2008; Stumm and Morgan, 2012). The latter assumption is often observed for freshwater systems as the concentrations of free surface sorption sites are generally much greater than concentrations of bound elements. However, the assumptions for reversibility and equilibrium are rarely verified because some sorption processes are poorly or

very slowly reversible. Therefore, we need to adapt the use of  $K_d$  values to the conditions of solid/liquid exchanges (e.g. adsorption, desorption, field) or the use of dynamic and/or mechanistic approaches.

For a single element,  $K_d$  distributions can cover several orders of magnitude. This variability is not surprising due to the complexity of solid-liquid exchanges and also to the empirical nature of this approach that can associate different sampling methods of the liquid and solid phases (section 2.1) and different measurement techniques to determine an element's content in different fractions (e.g. spectrometry for radionuclides, total or pseudo-total acid digestion of solids phases for stable nuclides). In freshwater environments such a large variability in values can cause problems since  $K_d$  is an important source of uncertainty in some radiological impact calculations involving dissolved and particulate elements in the water column and deposited sediments (Duchesne et al., 2003).

When specific  $K_d$  values are not available for modelling applications, modellers need reference  $K_d$  distributions. Therefore, the availability of such information is of great importance and has motivated the compilation of freshwater  $K_d$  values (Thibault et al., 1990; TRS 364; Allison and Allison, 2005; Durrieu et al., 2006; Ciffroy et al., 2009; TRS 422; TRS 472; Sheppard, 2011; IAEA 1994; IAEA 2001; IAEA 2010). The most recent compilations have been developed during EMRAS I by Durrieu and Ciffroy (Durrieu et al., 2006; Ciffroy et al., 2009; IAEA, 2010). The compilation gathers data from 86 references (essentially peer-reviewed publications) published before 2004 and includes freshwaters  $K_d$  values for 15 elements. Each  $K_d$  value recorded was associated with a wide range of parameters such as the source reference, location (river or lake name), type of sediment (deposited ( $DS$ ) or suspended ( $SS$ )), experimental conditions (ratio of solid mass to water volume ( $M/V$ ), contact time, sorption process and number of replicates), chemical conditions ( $pH$ , dissolved and particulate carbon, potassium and ammonium concentrations and ion exchange capacity) and the format of the presentation of data (e.g. figure, table).

For eight of these 15 elements (Ag, Am, Co, Cs, I, Mn, Pu and Sr) the datasets were large enough (defined by Durrieu et al. (2006) as at least ten data values originating from more than five different references) to allow the calculation of conditional log-normal distributions (geometric mean ( $GM$ ) and geometric standard deviation ( $GSD$ )) in three exchange conditions: adsorption, desorption and field (IAEA, 2010). The notion of field condition was introduced for two reasons: 1) it is difficult to clearly identify in the field if the solid/liquid exchange conditions are equilibrated and correspond to sorption or desorption whereas they are well controlled and identified in laboratories and 2) the temporal and spatial scales associated with  $K_d$  in the field are significantly larger than those associated with  $K_d$  obtained in the laboratory. For example, sorption/desorption experiments in the laboratory can cover several days or weeks, but rarely several months or years as is the case in the environment. For these reasons,  $K_d$  in the field are sometimes called “apparent  $K_d$ ” and hereafter have been termed here as  $K_{d(a)}$ .

For seven elements (Ba, Be, Ce, Ra, Ru, Sb and Th), the datasets were only sufficient (less than five references and/or less than ten  $K_d$  values) to determine non-conditional log-normal distributions. For a final third group of ten elements (Cr, Fe, Zn, Zr, Tc, Pm, Eu, U, Np and Cm), mean, maximum and minimum  $K_d$  values were suggested on the basis of a single publication (Onishi et al, 1991) or expert judgment.

To demonstrate the requirement to update and complete these previous compilations, Table 1 collates the 64 elements for which reference  $K_d$  values are required by the ERICA Tool for wildlife assessment (Brown et al., 2008) and the SYMBIOSE modelling platform for

environmental transfer and doses to human populations (Gonze et al., 2011; Simon-Cornu et al., 2015). We have specified a quality criteria for freshwater  $K_d$  for a range of elements with radioisotopes that are relevant for radiation protection and which are included in these two platforms (Table 1). The value of this criteria is defined as 3 when the underlying data is sufficient to produce conditional distributions, as 2 when the underlying data is sufficient to produce unconditional distributions, as 1 when the underlying data is based upon a single value provided by a single publication or an expert judgment and as 0 when there was no element-specific information identified.

**Table 1:** List of elements used in ERICA tool and SYMBIOSE platform based upon the quality criteria of available  $K_d$  values

Element	Quality criteria	Element	Quality criteria	Element	Quality criteria
<b>Ac</b>	0	<b>Fr</b>	1	<b>Pu</b>	3
<b>Ag</b>	3	<b>Gd</b>	0	<b>Ra</b>	3
<b>Am</b>	3	<b>H</b>	1	<b>Rb</b>	0
<b>As</b>	1	<b>Hg</b>	1	<b>Rh</b>	1
<b>At</b>	1	<b>I</b>	3	<b>Rn</b>	0
<b>Au</b>	0	<b>In</b>	1	<b>Ru</b>	3
<b>Ba</b>	3	<b>Ir</b>	0	<b>S</b>	1
<b>Be</b>	3	<b>La</b>	0	<b>Sb</b>	3
<b>Bi</b>	1	<b>Mn</b>	3	<b>Se</b>	1
<b>Br</b>	0	<b>Mo</b>	1	<b>SS</b>	1
<b>C</b>	1	<b>Na</b>	1	<b>Sn</b>	1
<b>Ca</b>	1	<b>Nb</b>	1	<b>Sr</b>	3
<b>Cd</b>	0	<b>Nd</b>	0	<b>Tc</b>	1
<b>Ce</b>	3	<b>Ni</b>	1	<b>Te</b>	1
<b>Cf</b>	0	<b>Np</b>	2	<b>Th</b>	3
<b>Cl</b>	1	<b>P</b>	0	<b>Tl</b>	1
<b>Cm</b>	2	<b>Pa</b>	0	<b>U</b>	2
<b>Co</b>	3	<b>Pb</b>	1	<b>W</b>	0
<b>Cr</b>	1	<b>Pd</b>	0	<b>Y</b>	1
<b>Cs</b>	3	<b>Pm</b>	2	<b>Zn</b>	2
<b>Eu</b>	2	<b>Po</b>	1	<b>Zr</b>	2
<b>Fe</b>	2	<b>Pr</b>	1		

Table 1 shows that 23% of the elements have a score of 3 and are conditional  $K_d$  distributions, 13% have a score of 2 and are unconditional  $K_d$  distributions, 42% have a score of 1 and are based upon a single  $K_d$  source or expert judgement, and 23% have a 0 score have no values. Therefore, 65% of elements in table 1 are based upon only a single value, expert judgment or are not associated with any  $K_d$  value.

The analysis clearly demonstrates the need to regularly update  $K_d$  compilations with the aim to fill the numerous gaps, especially for those elements for which contributions to dose for humans or other organisms are potentially important.

The aim of freshwater  $K_d$  related activities within WG4 of the MODARIA program was to enhance the EMRAS I compilations of  $K_d$  in freshwater environments to allow an update of  $K_d$  distributions published in TRS 472 (IAEA, 2010). The article is divided into three sections presenting: 1) an updated and completed dataset of freshwater  $K_d$ , 2) the analysis methodology of the enhanced dataset and 3) analysis of  $K_d$  distributions as a function of suspended and deposited sediments, suspended load and conditions of solid-liquid exchange.

## 2. MATERIALS AND METHODS

### 2.1. ENHANCEMENT OF THE FRESHWATER $K_d$ DATASET

Ciffroy kindly supplied the freshwater  $K_d$  dataset, from which the  $K_d$  distributions published in TRS 472 (IAEA, 2010) were derived to MODARIA WG4. The dataset was then expanded giving priority to elements for which there were few or no data. Major stable elements inputs included were from large datasets published by the US Geological Survey (USGS) for Colorado River (<http://pubs.usgs.gov/ds/614/contents/>), the Geochemical Atlas of Europe (<http://weppi.gtk.fi/publ/foregsatlas/>) and water quality data from 26 Ribble and Wyre river basin sites in North West England (Neal et al., 1997; Neal, 2007; Neal et al., 2011). New  $K_d$  values were also derived from peer reviewed publications for both radionuclides and stable elements. Over 2300 new  $K_d$  values were compiled for 27 new elements (Al, As, B, Ca, Cd, Cu, Dy, Er, Gd, Hf, Ho, K, La, Li, Mg, Mo, Na, Ni, Pb, Pr, Rb, S, Se, Si, Sn, Ti and V) which were added to those in the TRS 472 dataset. A total of 270 new  $K_d$  values were also added for the 25 elements already included in the TRS 472 dataset (Ag, Am, Ba, Be, Ce, Cm, Co, Cr, Cs, Eu, Fe, I, Mn, Np, Pm, Pu, Ra, Ru, Sb, Sr, Tc, Th, U, Zn, Zr). In TRS 472, ten elements have too few data values to derive lognormal distributions. The MODARIA dataset now provides adequate data to derive lognormal distributions for Cm, Cr, Eu, Fe, U and Zn. The values for the other four elements (Np, Pm, Tc and Zr) were not updated and remain the same as those in TRS 472 (IAEA, 2010).

In freshwater environments, the  $K_d$  approach can be applied to both suspended and/or deposited sediments. Reference documents such as TRS 472 do not distinguish  $K_d$  distributions between these two components. However, there is evidence, discussed below, that this omission needs to be addressed.

Suspended sediments are solid particles which are maintained in suspension in the water column to differing extents depending on their size and density, and the water flow conditions. The mean particle size of suspended sediments increases when the water flow increases (Mehta, 2014) and, as a consequence,  $K_d$  values of less soluble elements can decrease whereas they can increase for soluble elements (Abril and Fraga, 1996; IAEA, 2001; He and Walling, 1996). Therefore, it follows that hydro-sedimentary conditions can significantly contribute to the variability of the  $K_d$  values of suspended sediments.

Furthermore, suspended sediments can be sampled by different methods such as filtration, sediment traps located in the waterflow, sedimentation and centrifugation. These different methods also contribute to the variability of  $K_d$  values because they are characterized by different particle size cut-off values that lead to significant differences in the sampling of liquid and solid phases. For example,  $K_d$  values obtained by direct filtration are higher than  $K_d$  values determined by sediment traps which are less efficient at sampling the finest suspended particles which are more contaminated (Eyrolle et al., 2016). After sampling,  $K_d$  values can be determined according to three methods: batch experiments for adsorption and/or desorption conditions and direct measurements in the field of an element's concentration in filtered water and solid particles. Thus, the variability of  $K_d$  for suspended matter is not only dependent on the physico-chemical properties of an element, suspended particles and solutions, but also on the hydro-sedimentary conditions and the sampling and measuring methods.

Deposited sediments are mixtures of water and particles accumulated on the bottom of lakes or rivers by bed load and sedimentation of coarser suspended particles. The mean size of their particles is greater than that of suspended sediments and the contact surface between water and particles decreases when the porosity decreases. As for suspended particles, the different methods applied to determine their  $K_d$  values are a significant source of  $K_d$  variability. After sampling,  $K_d$  values can be experimentally obtained by suspension of deposited particles in batch experiments for adsorption and/or desorption conditions or by direct measurement in the field when an element's concentration is high enough to be measured. In this last case, two ratio approaches are usually applied between: 1) element concentration in dried bottom sediments and the water column and 2) element concentration in deposited particles and pore water.

To investigate these approaches, some fundamental aspects of the deposited sediments have been considered. A key aspect to consider is that the transfer of pollutants from the water column to the deposited sediments is dominated by the sedimentation of contaminated suspended particles and by diffusion between the contaminated water of the water column and the pore water of the superficial sediments. In the sediments, the accumulation of deposited particles creates sedimentary columns of superimposed layers constituting mixtures of particles and water which are submitted to several diagenetic processes (Boudreau, 1997) involving chemical reactions and vertical transfers by interstitial diffusion and/or bioturbation. The weight accumulated by these superimposed layers decreases the porosity with the sediment thickness and reduces the exchange between the pore water and the water column. Consequently, the sediments layers located under the superficial sediments become anoxic because their dissolved oxygen is more rapidly consumed by bacteria than it is replaced by interstitial diffusion with the free water. Thus, deposited sediments must be considered as two distinct domains: 1) an oxygenated fine superficial layer (1 to 2 centimetres) in contact with free water and 2) an anoxic layer which is weakly reactive to changes in the water column and that conserves the "memory" of the state of contamination when they first became anoxic. These processes explain why contamination profiles of cores of sediment are useful to rebuild the history of the contamination of freshwater systems.

Under these conditions, approach 1 can only be used for assessment of an element's concentration in the oxygenated superficial layer of deposited sediments assuming equilibrium conditions with the element's concentration in the water column. Ideally, this approach is only significant when all the particles of this layer have been accumulated during a period where the contamination of the water column can be assumed to be constant or when elemental concentrations in the pore water of bottom sediments are in equilibrium with those in the water column. Such an assumption limits its use to yearly or several monthly periods

and does not permit its application in the case of accidental or transitory situations such as that illustrated by Figure 1 for a pulse input of a polluting element.

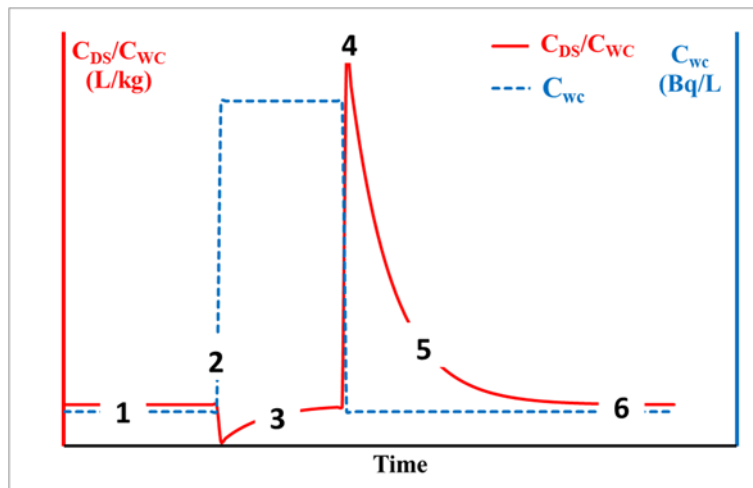


**Figure 1:** Ratio between the element concentration in superficial dried deposited sediments ( $C_{DS}$ ) with that in the water column ( $C_{wc}$ ) for a pulse input of a pollutant element

In Figure 1, before the arrival of the pulse (1), the water column and the deposited sediments are equilibrated and the ratio corresponds to the  $K_d$  value. Upon the arrival of the pulse (2), the ratio decreases strongly because the water column is contaminated, but the bottom sediments are not. Under these circumstances the ratio does not correspond to a  $K_d$  value. During the passing of the pulse (3), the ratio increases as a function of the sedimentation rate and will correspond to a  $K_d$  value only if the passing time of the pulse is long enough to reach equilibrium conditions. At the end of the pulse (4), the ratio increases strongly because the pollutant element concentration in the water column decreases significantly, while the sediment retains the element. Under these circumstances the ratio does not correspond to a  $K_d$  value. Thereafter (5), the ratio decreases slowly to reach the  $K_d$  value (6).

This illustration highlights that it is not possible to model such situations with a constant  $K_d$  value representative of the ratio between the element concentration of deposited sediments and the water column. For such situations, the ratio of the element concentration of superficial deposited sediment and pore water (approach 2) is more relevant but is rarely applied because it is more difficult to measure and to use in models. Measuring extracted pore water is difficult and, for modelling, the element concentration of deposited sediments cannot be directly deduced from the water column. Reactive kinetic models simulating several processes (sedimentation rate of suspended particles, kinetics of solid/liquid exchanges, interstitial diffusion, bioturbation...) are then more appropriate.

From these considerations, WG4 determined  $K_d$  distributions not only with regard to sorption-desorption processes and field measurements, as in TRS 472 (IAEA, 2010), but also as a function of suspended and deposited sediments. To do this,  $K_d$  distributions of each element were determined for six categories defined by the combinations between two components (suspended and deposited sediments) and three conditions of liquid-solid exchange (adsorption, desorption and field). The analysis incorporated:

- Elements reported in both MODARIA and TRS 472 (IAEA, 2010): Ag, Am, Ba, Be, Ce, Cm, Co, Cr, Cs, Eu, Fe, I, Mn, Pu, Ra, Ru, Sb, Sr, Th, U, Zn.

- New elements collated by MODARIA: Al, As, B, Ca, Cd, Cu, Dy, Er, Gd, Hf, Ho, K, La, Li, Mg, Mo, Na, Ni, Pb, Po, Pr, Rb, S, Se, Si, Sn, Ti, V.

## 2.2. METHOD OF ANALYSIS

The dataset of each chemical element was sub-divided according the type of sediment (suspended, deposited) and the solid-liquid exchange conditions (sorption, desorption, field). The analysis of each combination (element  $\times$  component  $\times$  condition) depended on the number of values,  $N$ .

- If  $N < 10$ , the distribution was not determined and the  $K_d$  value was provided for indication only and without statistical information. Two cases were possible:
  - $N = 1$ : only one value was given.
  - $N > 1$ : the geometric mean, the minimum and the maximum values of the dataset was reported.
- If  $N \geq 10$ , it was assumed that the dataset followed a lognormal distribution which was considered as the most appropriate approach when the data range was over several orders of magnitude, as it is often the case for  $K_d$  (Sheppard, 2011). The parameters reported for the distribution were the geometric mean ( $GM$ ), and the geometric standard deviation ( $GSD$ ). They were obtained by fitting the empirical cumulative distribution function ( $CDF$ ) with the log-normal cumulative distribution function ( $CDF^*$ ). The representiveness of this adjustment was assessed using the Kolmogorov-Smirnov statistical test (KS-test).

## 2.3. CONFIDENCE INDICATORS

An empirical confidence indicator ( $CI$ ) was associated to each  $K_d$  distribution to provide users with an indication of the level of confidence they could have for the reported values. The  $CI$  incorporated different criteria based on (i) the statistical properties of the datasets, (ii) some empirical assumptions about  $K_d$  behavior which were checked by comparing the statistical  $K_d$  distributions with the statistical Student t-test and (iii) comparisons with reference  $K_d$  values already published in previous documents. For each distribution,  $CI$  was initiated at 1 and was increased by 1 if  $N \geq 10$  and by 1 again if the KS-test was validated. The  $CI$  of the distributions checking the KS-test were incremented as a function of several empirical assumptions as follows:

1. For each condition of liquid – solid exchange (adsorption, desorption and field), it was assumed that the  $K_d$  distributions were greater for suspended sediments than for deposited sediments.  $CI$  was then increased by 1 for the distributions that conformed with one of the following criteria:

$$\begin{aligned} CDF(K_{dDS}^{ads}) &< CDF(K_{dSS}^{ads}) \\ CDF(K_{dDS}^{des}) &< CDF(K_{dSS}^{des}) \\ CDF(K_{dDS}^{fld}) &< CDF(K_{dSS}^{fld}) \end{aligned}$$

2. For the same component, it was assumed that the  $K_d$  distributions were lower for adsorption than for desorption and that  $K_d$  distributions for desorption were similar or lower than  $K_d$  distributions in the field.  $CI$  was then increased by 1 for the distributions that conformed with one of the following criteria:

$$\begin{aligned}
& CDF(K_{d_{SS}}^{ads}) < CDF(K_{d_{SS}}^{des}); CDF(K_{d_{SS}}^{ads}) < CDF(K_{d_{SS}}^{fld}) \\
& CDF(K_{d_{SS}}^{des}) \leq CDF(K_{d_{SS}}^{fld}); CDF(K_{d_{DS}}^{ads}) < CDF(K_{d_{DS}}^{des}) \\
& CDF(K_{d_{DS}}^{ads}) < CDF(K_{d_{DS}}^{fld}); CDF(K_{d_{DS}}^{des}) \leq CDF(K_{d_{DS}}^{fld})
\end{aligned}$$

3. The conditional  $K_d$  distributions given in TRS 472 (IAEA, 2010) do not distinguish SS and DS. For the same condition of liquid-solid exchange, it was assumed that the  $K_d$  distributions for SS and DS were respectively greater and lower than those of TRS 472. CI of the distributions were increased by 0.75 when they conformed with one of the following criteria:

$$\begin{aligned}
& CDF(K_{d_{DS}}^{ads}) < CDF(K_{d_{TRS}}^{ads}); CDF(K_{d_{DS}}^{des}) < CDF(K_{d_{TRS}}^{des}) \\
& CDF(K_{d_{DS}}^{fld}) < CDF(K_{d_{TRS}}^{fld}); CDF(K_{d_{TRS}}^{ads}) < CDF(K_{d_{SS}}^{ads}) \\
& CDF(K_{d_{TRS}}^{des}) < CDF(K_{d_{SS}}^{des}); CDF(K_{d_{TRS}}^{fld}) < CDF(K_{d_{SS}}^{fld})
\end{aligned}$$

4. The unconditional  $K_d$  distributions reported by TRS 472 (IAEA, 2010) aggregated all components and all exchange conditions. Assuming that the influence of the components is more important than the influence of exchange conditions, the CI of the  $K_d$  distributions for SS and DS were increased by 0.5 when they were respectively greater and lower than the unconditional distributions. The criteria are summarized as:

$$\begin{aligned}
& CDF(K_{d_{DS}}^{ads}) \leq CDF(K_{d_{TRS}}); CDF(K_{d_{DS}}^{des}) \leq CDF(K_{d_{TRS}}); CDF(K_{d_{DS}}^{fld}) \leq CDF(K_{d_{TRS}}) \\
& CDF(K_{d_{TRS}}) \leq CDF(K_{d_{SS}}^{ads}); CDF(K_{d_{TRS}}) \leq CDF(K_{d_{SS}}^{des}); CDF(K_{d_{TRS}}) \leq CDF(K_{d_{SS}}^{fld})
\end{aligned}$$

For some elements, TRS 472 (IAEA, 2010) provided only screening values. To take these values into account, CI was increased by 0.25 when the GM value of a distribution differed by less than a factor 10 from the screening value given in TRS 472 for the same element.

$$\begin{aligned}
& 0.1 \leq \left| \frac{GM(K_{d_{DS}}^{ads})}{K_{d_{TRS}}} \right| \leq 10; 0.1 \leq \left| \frac{GM(K_{d_{DS}}^{des})}{K_{d_{TRS}}} \right| \leq 10 \\
& 0.1 \leq \left| \frac{GM(K_{d_{DS}}^{fld})}{K_{d_{TRS}}} \right| \leq 10; 0.1 \leq \left| \frac{GM(K_{d_{SS}}^{ads})}{K_{d_{TRS}}} \right| \leq 10 \\
& 0.1 \leq \left| \frac{GM(K_{d_{SS}}^{des})}{K_{d_{TRS}}} \right| \leq 10; 0.1 \leq \left| \frac{GM(K_{d_{SS}}^{fld})}{K_{d_{TRS}}} \right| \leq 10
\end{aligned}$$

5. Without considerations of the exchange conditions, Allison and Allison (2005) published median  $K_d$  values for SS and DS. For these data, CI was increased by 0.5 when the GM value of a distribution differed by less than a factor of 10 from the median value given by Allison and Allison (2005) for the same component.

$$\begin{aligned}
& 0.1 < \frac{GM(K_{d_{DS}}^{ads})}{K_{d_{DS}}^{Allison}} < 10; 0.1 \leq \frac{GM(K_{d_{DS}}^{des})}{K_{d_{DS}}^{Allison}} < 10 \\
& 0.1 \leq \frac{GM(K_{d_{DS}}^{fld})}{K_{d_{DS}}^{Allison}} < 10; 0.1 \leq \frac{GM(K_{d_{SS}}^{ads})}{K_{d_{SS}}^{Allison}} < 10 \\
& 0.1 \leq \frac{GM(K_{d_{SS}}^{des})}{K_{d_{SS}}^{Allison}} < 10; 0.1 \leq \frac{GM(K_{d_{SS}}^{fld})}{K_{d_{SS}}^{Allison}} < 10
\end{aligned}$$

6. After each of the above steps, CI was normalized to its maximum possible value which is 7.25:

$$CI = CI/7.25$$

$$\text{Equation 2}$$

### 3. RESULTS

Table 2 reports the *GM*, *GSD*, maximum and minimum values, the 5<sup>th</sup> and 95<sup>th</sup> percentiles, the size of the dataset, the number of reference, the result of the KS-test and the *CI* value for 49 chemical elements.

**Table 2:**  $K_d$  distributions in function of environmental components (*SS* and *DS*) and conditions of liquid-solid exchange (adsorption, desorption, field)

Element	Component	Condition	<i>GM</i> L/kg	<i>GSD</i>	Min L/Kg	Max L/kg	5% L/Kg	95% L/Kg	Nd	Nr	K-S test	<i>CI</i>
Ag	DS	Field[0]	5.25×10 <sup>2</sup>	n.a	n.a	n.a	n.a	n.a	1	1	n.r	0.14
Ag	SS	Adsorption	8.30×10 <sup>4</sup>	2.28	1.21×10 <sup>4</sup>	1.58×10 <sup>6</sup>	2.14×10 <sup>4</sup>	3.22×10 <sup>5</sup>	81	7	OK	0.62
Ag	SS	Desorption	4.10×10 <sup>5</sup>	1.73	5.97×10 <sup>4</sup>	9.48×10 <sup>5</sup>	1.66×10 <sup>5</sup>	1.01×10 <sup>6</sup>	41	2	OK	0.62
Ag	SS	Field[0]	4.85×10 <sup>5</sup>	n.r	1.08×10 <sup>5</sup>	1.26×10 <sup>6</sup>	n.r	n.r	7	2	n.r	0.14
Al	SS	Field[0]	4.62×10 <sup>6</sup>	n.r	4.62×10 <sup>6</sup>	2.75×10 <sup>8</sup>	n.r	n.r	2	1	n.r	0.14
Am	DS	Adsorption	2.20×10 <sup>5</sup>	3.81	2.70×10 <sup>3</sup>	2.25×10 <sup>6</sup>	2.44×10 <sup>4</sup>	1.98×10 <sup>6</sup>	88	4	OK	0.41
Am	SS	Field[1]	7.94×10 <sup>4</sup>	6.25	1.10×10 <sup>3</sup>	1.31×10 <sup>6</sup>	3.90×10 <sup>3</sup>	1.62×10 <sup>6</sup>	44	4	OK	0.41
As	DS	Field[0]	4.26×10 <sup>3</sup>	3.47	6.50×10 <sup>1</sup>	2.93×10 <sup>4</sup>	5.51×10 <sup>2</sup>	3.29×10 <sup>4</sup>	35	7	OK	0.55
As	SS	Field[0]	1.63×10 <sup>4</sup>	2.88	9.32×10 <sup>1</sup>	2.36×10 <sup>5</sup>	2.86×10 <sup>3</sup>	9.30×10 <sup>4</sup>	50	6	OK	0.62
B	SS	Field[1]	1.41×10 <sup>3</sup>	2.56	4.42×10 <sup>2</sup>	6.20×10 <sup>3</sup>	2.99×10 <sup>2</sup>	6.62×10 <sup>3</sup>	21	1	OK	0.41
Ba	DS	Field[0]	8.13×10 <sup>3</sup>	n.r	8.13×10 <sup>3</sup>	1.05×10 <sup>4</sup>	n.r	n.r	2	2	n.r	0.14
Ba	DS	Adsorption	3.95×10 <sup>2</sup>	n.r	4.50×10 <sup>1</sup>	5.50×10 <sup>2</sup>	n.r	n.r	8	1	n.r	0.14
Ba	SS	Adsorption	1.75×10 <sup>3</sup>	3.18	7.20×10 <sup>2</sup>	5.74×10 <sup>3</sup>	2.61×10 <sup>2</sup>	1.17×10 <sup>4</sup>	11	2	OK	0.62
Ba	SS	Field[2]	7.95×10 <sup>3</sup>	2.75	8.48×10 <sup>2</sup>	7.84×10 <sup>4</sup>	1.50×10 <sup>3</sup>	4.21×10 <sup>4</sup>	70	6	OK	0.62
Be	SS	Adsorption	1.60×10 <sup>5</sup>	n.r	1.60×10 <sup>5</sup>	3.60×10 <sup>5</sup>	n.r	n.r	2	1	n.r	0.14
Be	SS	Field[0]	3.87×10 <sup>4</sup>	2.59	2.20×10 <sup>3</sup>	2.00×10 <sup>5</sup>	8.06×10 <sup>3</sup>	1.85×10 <sup>5</sup>	29	6	OK	0.48
Ca	DS	Field[0]	1.38×10 <sup>2</sup>	n.r	5.42×10 <sup>1</sup>	1.47×10 <sup>3</sup>	n.r	n.r	3	2	n.r	0.14
Ca	SS	Field[1]	1.35×10 <sup>3</sup>	1.44	4.12×10 <sup>2</sup>	5.50×10 <sup>3</sup>	7.38×10 <sup>2</sup>	2.46×10 <sup>3</sup>	23	3	OK	0.41
Cd	DS	Field[2]	3.29×10 <sup>2</sup>	6.48	7.69×10 <sup>1</sup>	1.50×10 <sup>4</sup>	1.52×10 <sup>1</sup>	7.12×10 <sup>3</sup>	14	4	OK	0.55
Cd	SS	Field[2]	6.78×10 <sup>4</sup>	2.07	1.65×10 <sup>3</sup>	2.40×10 <sup>5</sup>	2.06×10 <sup>4</sup>	2.24×10 <sup>5</sup>	33	6	OK	0.62
Ce	SS	Adsorption	1.81×10 <sup>5</sup>	n.r	5.30×10 <sup>4</sup>	9.21×10 <sup>5</sup>	n.r	n.r	6	1	n.r	0.14
Ce	SS	Field[4]	1.66×10 <sup>5</sup>	1.87	7.25×10 <sup>4</sup>	1.50×10 <sup>6</sup>	5.91×10 <sup>4</sup>	4.64×10 <sup>5</sup>	23	2	OK	0.41
Cm	DS	Adsorption	1.64×10 <sup>5</sup>	6.81	1.00×10 <sup>4</sup>	2.25×10 <sup>6</sup>	7.00×10 <sup>3</sup>	3.86×10 <sup>6</sup>	29	1	OK	0.41
Cm	SS	Field[0]	1.01×10 <sup>5</sup>	n.a	5.25×10 <sup>4</sup>	2.88×10 <sup>5</sup>	n.a	n.a	4	1	n.r	0.14
Co	DS	Adsorption	1.59×10 <sup>4</sup>	10.40	2.00×10 <sup>1</sup>	5.43×10 <sup>5</sup>	3.40×10 <sup>2</sup>	7.48×10 <sup>5</sup>	300	8	NO	0.28
Co	DS	Desorption	1.57×10 <sup>4</sup>	65.00	6.76×10 <sup>1</sup>	2.50×10 <sup>6</sup>	1.63×10 <sup>1</sup>	1.50×10 <sup>7</sup>	34	3	OK	0.72
Co	DS	Field[3]	8.55×10 <sup>1</sup>	28.30	2.00×10 <sup>0</sup>	1.40×10 <sup>5</sup>	3.50×10 <sup>-1</sup>	2.09×10 <sup>4</sup>	20	4	OK	0.66
Co	SS	Adsorption	8.76×10 <sup>4</sup>	13.8	2.79×10 <sup>2</sup>	1.13×10 <sup>7</sup>	1.17×10 <sup>3</sup>	6.56×10 <sup>6</sup>	234	16	OK	0.72
Co	SS	Desorption	1.10×10 <sup>6</sup>	5.05	1.20×10 <sup>4</sup>	1.54×10 <sup>7</sup>	7.71×10 <sup>4</sup>	1.58×10 <sup>7</sup>	40	2	OK	0.79
Co	SS	Field[3]	4.43×10 <sup>4</sup>	2.47	3.70×10 <sup>3</sup>	9.26×10 <sup>5</sup>	1.00×10 <sup>4</sup>	1.96×10 <sup>5</sup>	75	11	OK	0.62
Cr	DS	Field[3]	1.76×10 <sup>4</sup>	14.30	2.92×10 <sup>2</sup>	1.29×10 <sup>5</sup>	2.21×10 <sup>2</sup>	1.41×10 <sup>6</sup>	25	4	OK	0.55
Cr	SS	Field[3]	6.87×10 <sup>4</sup>	1.74	1.23×10 <sup>3</sup>	6.10×10 <sup>5</sup>	2.76×10 <sup>4</sup>	1.71×10 <sup>5</sup>	54	7	OK	0.55
Cs	DS	Adsorption	4.97×10 <sup>3</sup>	9.74	9.92×10 <sup>0</sup>	6.06×10 <sup>4</sup>	1.18×10 <sup>2</sup>	2.10×10 <sup>5</sup>	366	10	NO	0.28
Cs	DS	Desorption	1.35×10 <sup>4</sup>	5.67	8.37×10 <sup>2</sup>	2.10×10 <sup>5</sup>	7.76×10 <sup>2</sup>	2.33×10 <sup>5</sup>	55	3	NO	0.28
Cs	DS	Field[3]	6.66×10 <sup>3</sup>	3.91	7.25×10 <sup>2</sup>	2.47×10 <sup>5</sup>	7.06×10 <sup>2</sup>	6.28×10 <sup>4</sup>	55	7	OK	0.66
Cs	SS	Adsorption	1.71×10 <sup>4</sup>	2.47	1.25×10 <sup>3</sup>	1.37×10 <sup>5</sup>	3.86×10 <sup>3</sup>	7.58×10 <sup>4</sup>	203	15	OK	0.66
Cs	SS	Desorption	3.30×10 <sup>4</sup>	2.50	4.36×10 <sup>3</sup>	1.38×10 <sup>5</sup>	7.30×10 <sup>3</sup>	1.49×10 <sup>5</sup>	64	4	OK	0.14
Cs	SS	Field[2]	1.35×10 <sup>5</sup>	2.67	2.34×10 <sup>3</sup>	2.70×10 <sup>6</sup>	2.64×10 <sup>4</sup>	6.69×10 <sup>5</sup>	211	13	OK	0.79
Cu	DS	Field[0]	7.28×10 <sup>3</sup>	21.40	4.40×10 <sup>0</sup>	2.94×10 <sup>5</sup>	4.71×10 <sup>1</sup>	1.13×10 <sup>6</sup>	62	15	NO	0.28
Cu	SS	Field[0]	3.26×10 <sup>4</sup>	2.19	1.05×10 <sup>2</sup>	9.59×10 <sup>6</sup>	8.96×10 <sup>3</sup>	1.18×10 <sup>5</sup>	69	14	OK	0.48
Dy	DS	Field[3]	5.80×10 <sup>5</sup>	2.53	4.07×10 <sup>4</sup>	3.66×10 <sup>6</sup>	1.26×10 <sup>5</sup>	2.66×10 <sup>6</sup>	26	1	OK	0.41
Er	DS	Field[3]	4.85×10 <sup>5</sup>	2.24	4.28×10 <sup>4</sup>	3.24×10 <sup>6</sup>	1.28×10 <sup>5</sup>	1.83×10 <sup>6</sup>	26	1	OK	0.41
Eu	DS	Field[3]	2.10×10 <sup>5</sup>	2.18	2.69×10 <sup>4</sup>	6.52×10 <sup>5</sup>	5.81×10 <sup>4</sup>	7.57×10 <sup>5</sup>	29	1	OK	0.41
Fe	DS	Field[0]	3.28×10 <sup>3</sup>	69.10	1.05×10 <sup>1</sup>	5.00×10 <sup>6</sup>	3.09×10 <sup>0</sup>	3.47×10 <sup>6</sup>	32	9	OK	0.55
Fe	SS	Field[0]	1.57×10 <sup>5</sup>	2.74	2.41×10 <sup>3</sup>	3.51×10 <sup>6</sup>	2.99×10 <sup>4</sup>	8.22×10 <sup>5</sup>	56	9	OK	0.55
Gd	DS	Field[3]	4.26×10 <sup>5</sup>	3.16	3.51×10 <sup>4</sup>	4.35×10 <sup>6</sup>	6.43×10 <sup>4</sup>	2.82×10 <sup>6</sup>	29	1	OK	0.41
Hf	DS	Field[3]	1.93×10 <sup>6</sup>	1.77	3.77×10 <sup>5</sup>	6.11×10 <sup>6</sup>	7.56×10 <sup>5</sup>	4.94×10 <sup>6</sup>	26	1	OK	0.41

Ho	DS	Field[3]	4.25×10 <sup>5</sup>	1.97	3.98×10 <sup>4</sup>	1.16×10 <sup>6</sup>	1.39×10 <sup>5</sup>	1.30×10 <sup>6</sup>	26	1	OK	0.41
I	DS	Adsorption	1.93×10 <sup>1</sup>	17.40	7.47×10 <sup>-2</sup>	4.00×10 <sup>3</sup>	1.75×10 <sup>-1</sup>	2.12×10 <sup>3</sup>	89	5	OK	0.66
I	SS	Adsorption	3.62×10 <sup>3</sup>	4.17	1.70×10 <sup>2</sup>	1.05×10 <sup>5</sup>	3.46×10 <sup>2</sup>	3.78×10 <sup>4</sup>	71	5	OK	0.55
I	SS	Field[0]	3.32×10 <sup>3</sup>	1.34	7.88×10 <sup>2</sup>	4.64×10 <sup>3</sup>	2.06×10 <sup>3</sup>	5.36×10 <sup>3</sup>	20	1	OK	0.41
K	SS	Field[1]	1.93×10 <sup>3</sup>	2.14	8.60×10 <sup>2</sup>	1.01×10 <sup>4</sup>	5.66×10 <sup>2</sup>	6.95×10 <sup>3</sup>	21	1	OK	0.41
La	DS	Field[4]	1.03×10 <sup>6</sup>	2.49	3.72×10 <sup>4</sup>	1.80×10 <sup>7</sup>	2.31×10 <sup>5</sup>	4.64×10 <sup>6</sup>	32	2	OK	0.41
La	SS	Field[4]	1.36×10 <sup>5</sup>	1.69	7.01×10 <sup>4</sup>	4.09×10 <sup>5</sup>	5.73×10 <sup>4</sup>	3.21×10 <sup>5</sup>	21	1	OK	0.41
Li	DS	Field[3]	7.60×10 <sup>3</sup>	2.08	9.32×10 <sup>1</sup>	5.01×10 <sup>4</sup>	2.28×10 <sup>3</sup>	2.54×10 <sup>4</sup>	32	1	OK	0.41
Mg	DS	Field[0]	1.33×10 <sup>2</sup>	n.r	6.25×10 <sup>1</sup>	3.04×10 <sup>2</sup>	n.r	n.r	8	1	n.r	0.14
Mg	SS	Field[2]	1.63×10 <sup>3</sup>	1.64	8.45×10 <sup>1</sup>	4.69×10 <sup>3</sup>	7.26×10 <sup>2</sup>	3.68×10 <sup>3</sup>	24	3	OK	0.41
Mn	DS	Adsorption	5.50×10 <sup>3</sup>	50.30	5.33×10 <sup>1</sup>	1.64×10 <sup>6</sup>	8.74×10 <sup>0</sup>	3.46×10 <sup>6</sup>	69	2	OK	0.83
Mn	DS	Desorption	5.94×10 <sup>3</sup>	n.r	1.87×10 <sup>3</sup>	1.64×10 <sup>6</sup>	n.r	n.r	6	1	n.r	0.14
Mn	DS	Field[1]	2.97×10 <sup>4</sup>	11.30	3.70×10 <sup>2</sup>	3.42×10 <sup>6</sup>	5.52×10 <sup>2</sup>	1.60×10 <sup>6</sup>	38	6	OK	0.83
Mn	SS	Adsorption	2.39×10 <sup>5</sup>	9.75	3.73×10 <sup>3</sup>	2.01×10 <sup>7</sup>	5.63×10 <sup>3</sup>	1.01×10 <sup>7</sup>	127	14	OK	0.79
Mn	SS	Desorption	1.33×10 <sup>6</sup>	6.33	2.70×10 <sup>4</sup>	1.00×10 <sup>7</sup>	6.38×10 <sup>4</sup>	2.76×10 <sup>7</sup>	40	2	OK	0.55
Mn	SS	Field[0]	7.21×10 <sup>4</sup>	3.15	1.63×10 <sup>3</sup>	2.20×10 <sup>8</sup>	1.09×10 <sup>4</sup>	4.76×10 <sup>5</sup>	75	13	OK	0.55
Mo	DS	Field[0]	7.27×10 <sup>1</sup>	n.r	4.16×10 <sup>1</sup>	2.69×10 <sup>2</sup>	n.r	n.r	3	2	n.r	0.14
Mo	SS	Field[1]	6.07×10 <sup>3</sup>	3.09	8.08×10 <sup>-1</sup>	7.11×10 <sup>6</sup>	9.48×10 <sup>2</sup>	3.89×10 <sup>4</sup>	29	2	OK	0.41
Na	SS	Field[3]	1.53×10 <sup>3</sup>	1.48	4.37×10 <sup>2</sup>	4.29×10 <sup>3</sup>	8.01×10 <sup>2</sup>	2.92×10 <sup>3</sup>	22	1	OK	0.41
Ni	DS	Field[3]	1.03×10 <sup>3</sup>	5.99	1.87×10 <sup>1</sup>	5.67×10 <sup>4</sup>	5.41×10 <sup>1</sup>	1.96×10 <sup>4</sup>	39	10	OK	0.55
Ni	SS	Field[3]	1.86×10 <sup>4</sup>	3.77	8.69×10 <sup>2</sup>	5.40×10 <sup>5</sup>	2.10×10 <sup>3</sup>	1.65×10 <sup>5</sup>	59	11	OK	0.62
Pb	DS	Field[3]	4.18×10 <sup>4</sup>	14.90	3.33×10 <sup>1</sup>	5.60×10 <sup>6</sup>	4.91×10 <sup>2</sup>	3.56×10 <sup>6</sup>	29	9	OK	0.62
Pb	SS	Field[2]	2.63×10 <sup>5</sup>	2.30	1.14×10 <sup>4</sup>	1.66×10 <sup>7</sup>	6.66×10 <sup>4</sup>	1.04×10 <sup>6</sup>	70	16	OK	0.62
Po	DS	Field[2]	1.02×10 <sup>5</sup>	5.35	2.21×10 <sup>4</sup>	6.10×10 <sup>6</sup>	6.45×10 <sup>3</sup>	1.61×10 <sup>6</sup>	10	2	OK	0.55
Po	SS	Field[1]	8.42×10 <sup>5</sup>	28.70	6.60×10 <sup>4</sup>	2.58×10 <sup>7</sup>	3.37×10 <sup>3</sup>	2.10×10 <sup>8</sup>	10	3	OK	0.55
Pr	SS	Field[4]	1.21×10 <sup>5</sup>	1.77	5.37×10 <sup>4</sup>	4.21×10 <sup>5</sup>	4.73×10 <sup>4</sup>	3.11×10 <sup>5</sup>	21	1	OK	0.41
Pu	DS	Adsorption	6.49×10 <sup>4</sup>	2.78	9.30×10 <sup>3</sup>	4.20×10 <sup>5</sup>	1.21×10 <sup>4</sup>	3.48×10 <sup>5</sup>	33	3	OK	0.55
Pu	DS	Desorption	2.96×10 <sup>5</sup>	2.05	3.07×10 <sup>4</sup>	1.25×10 <sup>7</sup>	9.07×10 <sup>4</sup>	9.65×10 <sup>5</sup>	41	4	OK	0.55
Pu	SS	Adsorption	6.04×10 <sup>4</sup>	n.r	6.00×10 <sup>3</sup>	3.00×10 <sup>6</sup>	n.r	n.r	4	1	n.r	0.14
Pu	SS	Field[1]	1.47×10 <sup>5</sup>	13.90	2.00×10 <sup>2</sup>	1.60×10 <sup>7</sup>	1.94×10 <sup>3</sup>	1.11×10 <sup>7</sup>	79	6	OK	0.41
Ra	DS	Adsorption	8.18×10 <sup>3</sup>	1.30	5.63×10 <sup>3</sup>	2.42×10 <sup>4</sup>	5.33×10 <sup>3</sup>	1.26×10 <sup>4</sup>	10	1	OK	0.41
Ra	DS	Field[3]	1.20×10 <sup>3</sup>	23.90	8.24×10 <sup>1</sup>	1.67×10 <sup>5</sup>	6.49×10 <sup>0</sup>	2.22×10 <sup>5</sup>	15	4	OK	0.48
Ra	SS	Adsorption	1.18×10 <sup>4</sup>	n.r	6.30×10 <sup>3</sup>	2.42×10 <sup>4</sup>	n.r	n.r	9	1	n.r	0.14
Ra	SS	Field[3]	5.21×10 <sup>3</sup>	2.76	1.13×10 <sup>2</sup>	1.73×10 <sup>5</sup>	9.79×10 <sup>2</sup>	2.77×10 <sup>4</sup>	48	3	OK	0.41
Rb	SS	Field[1]	7.33×10 <sup>3</sup>	1.92	2.12×10 <sup>3</sup>	2.38×10 <sup>4</sup>	2.50×10 <sup>3</sup>	2.15×10 <sup>4</sup>	21	1	OK	0.41
Ru	DS	Adsorption	5.28×10 <sup>4</sup>	1.39	3.34×10 <sup>4</sup>	7.90×10 <sup>4</sup>	3.09×10 <sup>4</sup>	9.03×10 <sup>4</sup>	36	1	OK	0.41
Ru	SS	Field[0]	2.73×10 <sup>4</sup>	1.67	4.00×10 <sup>2</sup>	5.39×10 <sup>4</sup>	1.17×10 <sup>4</sup>	6.36×10 <sup>4</sup>	38	2	OK	0.41
S	SS	Field[1]	1.33×10 <sup>3</sup>	1.55	7.25×10 <sup>2</sup>	7.06×10 <sup>3</sup>	6.44×10 <sup>2</sup>	2.73×10 <sup>3</sup>	21	1	OK	0.41
Sb	DS	Field[0]	1.20×10 <sup>4</sup>	n.r	1.09×10 <sup>4</sup>	1.94×10 <sup>4</sup>	n.r	n.r	3	1	n.r	0.14
Sb	SS	Adsorption	6.75×10 <sup>3</sup>	2.73	8.00×10 <sup>2</sup>	4.00×10 <sup>4</sup>	1.29×10 <sup>3</sup>	3.52×10 <sup>4</sup>	16	2	OK	0.41
Sb	SS	Field[3]	8.14×10 <sup>3</sup>	2.64	3.40×10 <sup>1</sup>	1.03×10 <sup>5</sup>	1.65×10 <sup>3</sup>	4.01×10 <sup>4</sup>	44	8	OK	0.41
Se	DS	Field[0]	7.08×10 <sup>3</sup>	n.a	n.a	n.a	n.a	n.a	1	1	n.r	0.14
Se	SS	Field[1]	1.54×10 <sup>4</sup>	2.19	5.41×10 <sup>3</sup>	6.65×10 <sup>4</sup>	4.24×10 <sup>3</sup>	5.61×10 <sup>4</sup>	22	1	OK	0.41
Si	SS	Field[1]	5.79×10 <sup>3</sup>	1.88	2.42×10 <sup>3</sup>	1.25×10 <sup>4</sup>	2.05×10 <sup>3</sup>	1.64×10 <sup>4</sup>	21	1	OK	0.41
Sn	SS	Field[0]	1.33×10 <sup>5</sup>	1.59	3.72×10 <sup>4</sup>	3.41×10 <sup>5</sup>	6.18×10 <sup>4</sup>	2.86×10 <sup>5</sup>	21	1	OK	0.41
Sr	DS	Adsorption	5.01×10 <sup>1</sup>	3.21	2.84×10 <sup>0</sup>	1.34×10 <sup>3</sup>	7.34×10 <sup>0</sup>	3.42×10 <sup>2</sup>	126	5	NO	0.28
Sr	DS	Desorption	4.81×10 <sup>2</sup>	2.23	3.46×10 <sup>1</sup>	2.06×10 <sup>3</sup>	1.29×10 <sup>2</sup>	1.80×10 <sup>3</sup>	34	3	OK	0.41
Sr	DS	Field[0]	1.38×10 <sup>2</sup>	n.a	6.00×10 <sup>0</sup>	3.45×10 <sup>3</sup>	n.a	n.a	8	4	n.r	0.14
Sr	SS	Adsorption	1.42×10 <sup>3</sup>	1.34	4.80×10 <sup>2</sup>	2.48×10 <sup>3</sup>	8.76×10 <sup>2</sup>	2.30×10 <sup>3</sup>	30	2	OK	0.66
Sr	SS	Field[2]	2.96×10 <sup>3</sup>	3.79	1.11×10 <sup>2</sup>	1.99×10 <sup>4</sup>	3.31×10 <sup>2</sup>	2.65×10 <sup>4</sup>	39	5	OK	0.66
Th	DS	Adsorption	1.56×10 <sup>5</sup>	47.80	1.15×10 <sup>2</sup>	2.75×10 <sup>6</sup>	2.69×10 <sup>2</sup>	9.04×10 <sup>7</sup>	12	2	OK	0.41
Th	DS	Field[0]	7.40×10 <sup>2</sup>	n.a	3.60×10 <sup>2</sup>	4.72×10 <sup>5</sup>	n.a	n.a	9	3	n.r	0.14
Th	SS	Field[0]	1.52×10 <sup>5</sup>	2.90	1.13×10 <sup>4</sup>	1.60×10 <sup>6</sup>	2.64×10 <sup>4</sup>	8.76×10 <sup>5</sup>	41	4	OK	0.41
Ti	DS	Field[0]	4.07×10 <sup>4</sup>	n.a	n.a	n.a	n.a	n.a	1	1	n.r	0.14
Ti	SS	Field[2]	1.05×10 <sup>5</sup>	1.35	2.41×10 <sup>4</sup>	1.58×10 <sup>5</sup>	6.42×10 <sup>4</sup>	1.71×10 <sup>5</sup>	21	1	OK	0.41
U	DS	Field[2]	3.50×10 <sup>3</sup>	40.10	9.10×10 <sup>1</sup>	8.04×10 <sup>4</sup>	8.07×10 <sup>0</sup>	1.51×10 <sup>6</sup>	14	5	OK	0.41
U	SS	Field[1]	1.19×10 <sup>4</sup>	5.63	3.05×10 <sup>2</sup>	1.27×10 <sup>5</sup>	6.94×10 <sup>2</sup>	2.04×10 <sup>5</sup>	38	6	OK	0.41
V	DS	Field[0]	3.71×10 <sup>4</sup>	n.a	n.a	n.a	n.a	n.a	1	1	n.r	0.14
V	SS	Field[2]	4.29×10 <sup>4</sup>	1.40	1.19×10 <sup>4</sup>	8.46×10 <sup>4</sup>	2.47×10 <sup>4</sup>	7.44×10 <sup>4</sup>	21	1	OK	0.41
Zn	DS	Field[2]	1.49×10 <sup>2</sup>	32.40	2.11×10 <sup>0</sup>	1.71×10 <sup>4</sup>	4.89×10 <sup>-1</sup>	4.53×10 <sup>4</sup>	31	7	OK	0.55
Zn	SS	Field[2]	7.20×10 <sup>4</sup>	2.68	3.00×10 <sup>3</sup>	3.32×10 <sup>7</sup>	1.43×10 <sup>4</sup>	3.64×10 <sup>5</sup>	50	11	OK	0.62

(\*) indicates median values. No (\*) corresponds to geometric means.

Nd = number of data

Nr = number of references

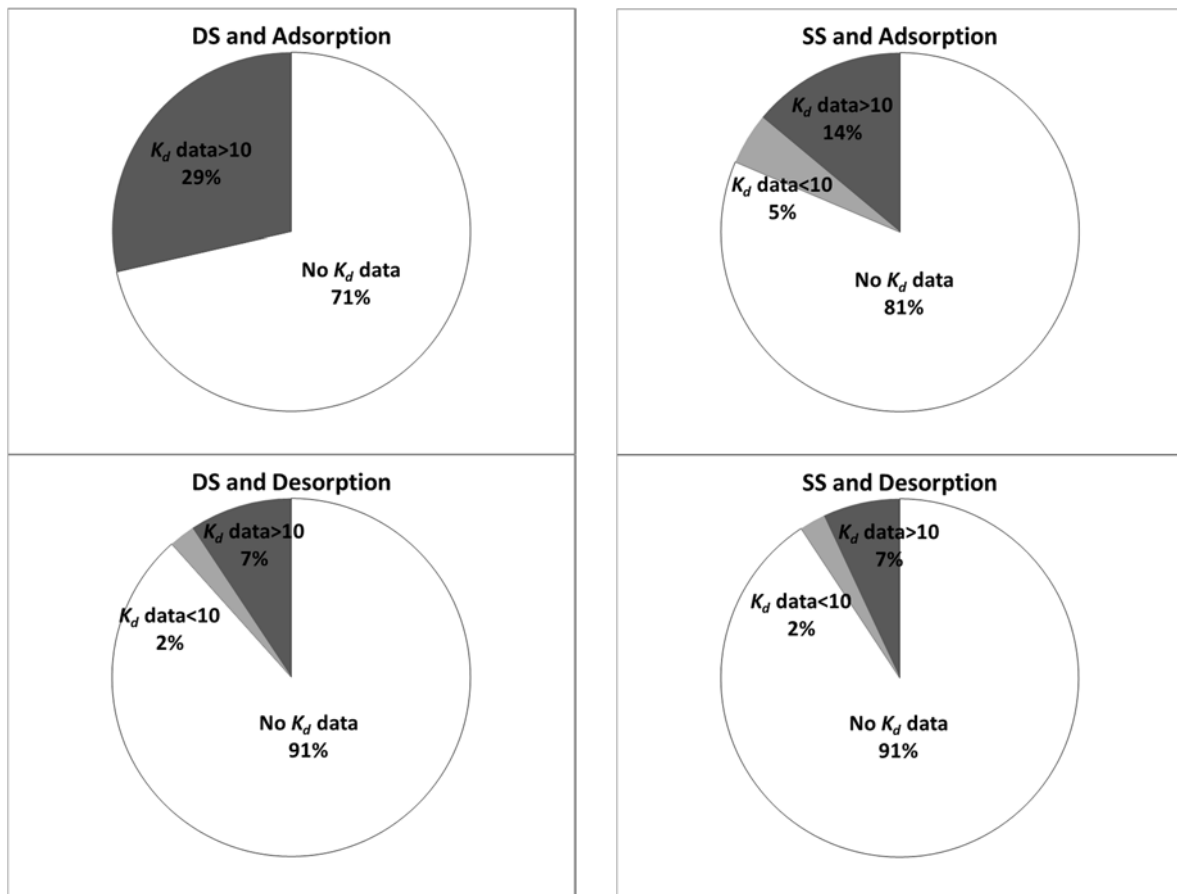
n.a = not available

n.r = not relevant

Field[X]: Representativeness of  $K_d$  datasets for field conditions (see 4.1 for SS and 4.2 for DS):  
Field[0]: no information; Field[1]: relevant for anthropic releases; Field[2]: relevant for anthropic releases with a risk of overestimation; Field[3] and Field[4]: relevant for environmental conditions.

For the 49 elements in table 2,  $K_d$  distributions should be available for all 294 combinations (49 elements x 2 components x 3 conditions). Including all new data, improved the number of elements and the assessment of the representativeness of the data. However,  $K_d$  data were still missing for 63% (186) of the possible combinations. For 7% (21) of the combinations, the datasets comprised less than 10  $K_d$  data and so only screening values were reported. On a more positive note, 30% (87) of the combinations were associated to  $K_d$  datasets with more than 10  $K_d$  values and their  $K_d$  distributions were reported.

For the 49 elements, Figure 3 shows how the data were distributed for each of the six combinations between the 2 components and the three conditions.



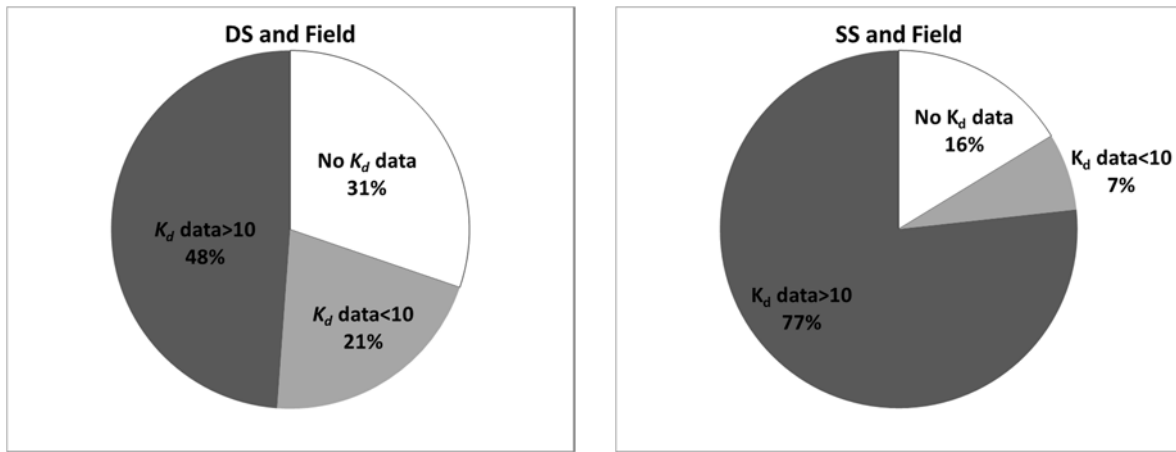


**Figure 2:** Distribution of the  $K_d$  datasets of the 49 listed elements for the six combinations between components and conditions

For the majority of the elements considered there were no reported  $K_d$  values for desorption and adsorption conditions for SS and DS. However, under field conditions SS and DS  $CI$  can be calculated. Figure 3 shows the  $CI$  arranged in increasing order.

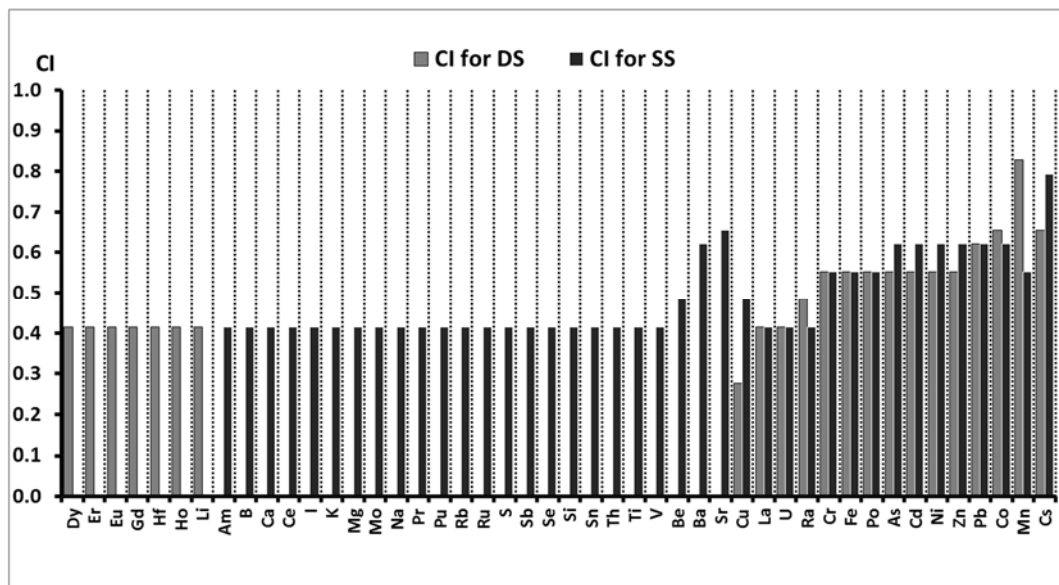


**Figure 3:**  $CI$  values for  $K_d$  distributions under field conditions

For field conditions, only four elements did not have reported  $K_d$  distributions (Ag, Al, Cm, Zr). Seven elements have  $K_d$  distributions for only DS (Dy, Er, Eu, Gd, Hf, Ho, Li) and 23 for only SS (Am, B, Ca, Ce, I, K, Mg, Mo, Na, Pr, Pu, Rb, Ru, S, Sb, Se, Si, Sn, Th, Ti, V, Be, Ba). Five elements (Sr, Cu, La, U, Ra) had  $K_d$  distributions for both SS and DS with  $CI$  values lower than 0.5. Eleven elements had calculated  $CI$  values greater than 0.5 for both SS and DS (Cr, Fe, Po, As, Cd, Ni, Zn, Pb, Co, Mn, Cs) and, therefore, there should be a greater confidence in the reported  $K_d$  values.

## 4. DISCUSSION

Three aspects of the revised  $K_d$  distributions are considered below.

### 4.1. $K_d$ DISTRIBUTIONS FOR $SS$ IN THE FIELD AS A FUNCTION OF THE MASS-VOLUME RATIO

Under field conditions, Table 2 demonstrates that most of the  $K_d$  distributions for  $SS$  were higher than those for  $DS$ . This can be attributed to the higher mean size of the deposited particles compared with that of suspended particles (IAEA, 2001). To revisit this assumption, it is relevant to analyse the behaviour of  $K_d$  values as a function of the mean particle size. Unfortunately, the mean particle size is rarely reported. Here, we have addressed this difficulty by analyzing the change in  $K_d$  values of  $SS$  in the field as a function of the  $M/V$  ratio. In rivers,  $M/V$  ratio corresponds to the suspended load  $[SS]$  which is frequently reported in the literature. It can be assumed that  $[SS]$  and the mean particle size of the suspended particles are roughly correlated as they both tend to increase at the same time when water flow increases (Metha, 2014; Müller and Förstener, 1968), although this behavior is not always observed (Walling et al., 2000). Thus, an apparent decrease of  $K_d$  values of suspended particles in the field is often observed when  $[SS]$  increases (Benoit et al., 1994; Honeyman and Santschi, 1988; Eyrolle et al., 2016). The  $K_d$  decrease can be explained by three mechanisms: (i) an increase of the mean particle size decreases the particulate element concentration, (ii) an increase of colloidal concentration that enriches the element concentration of the filtered water, this process is defined as the colloidal pumping (Benoit and Rozan, 1999) and (iii) high suspended load conditions can promote the aggregation of suspended particles and reduce the amount of exchange surfaces.

$K_d$  values for adsorption and desorption conditions were not included in our  $M/V$  analysis because they were obtained in laboratory conditions which did not consider the relationship between  $[SS]$  and particle sizes. For  $K_d$  values of  $SS$  in the field, only those values were considered that were associated with datasets with a  $CI$  above or equal to 0.4 and to a suspended load value. With these criterion, this analysis could be carried out for Am, As, B, Ba, Be, Ca, Cd, Ce, Co, Cr, Cs, Cu, Fe, K, La, Mg, Mn, Mo, Na, Ni, Pb, Po, Pr, Pu, Ra, Rb, S, Sb, Se, Si, Sn, Sr, Th, Ti, U, V and Zn.

For each element, the change in  $K_d$  as a function of  $[SS]$  was fitted with the following relationship (He and Walling, 1996):

$$K_d = a \cdot [SS]^b \quad \text{Equation 3}$$

An inverse behaviour between  $K_d$  and  $[SS]$  is obtained when  $b$  is negative as shown in Figure 4 for Cs, Am, Pu and Sr.

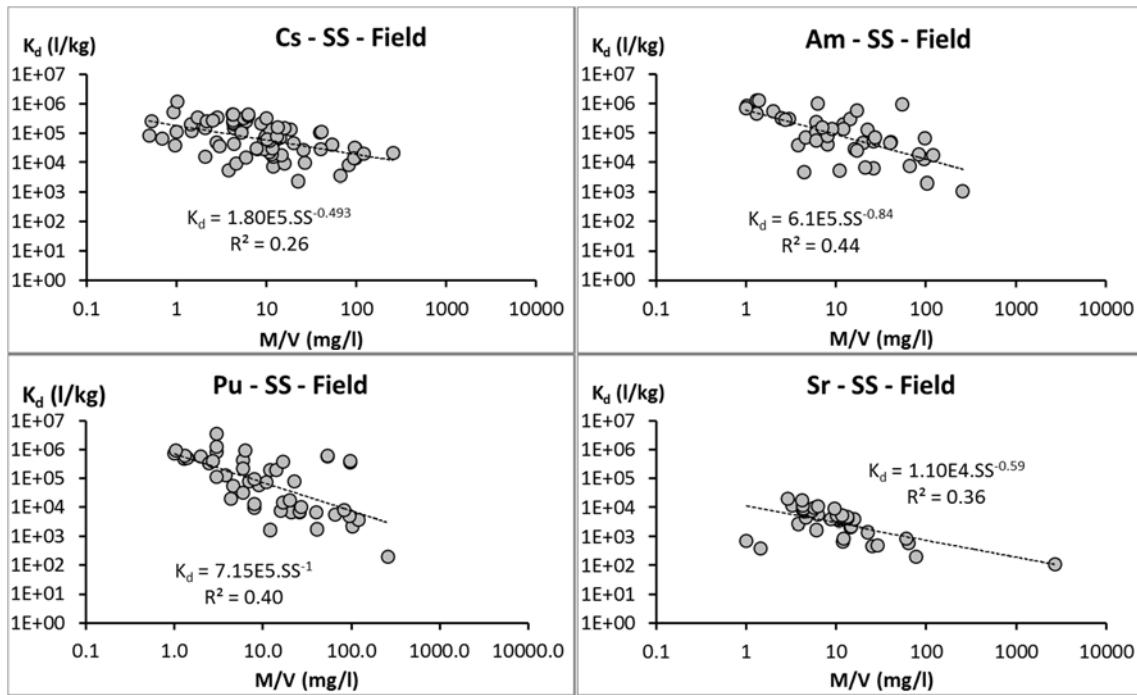


**Figure 4:**  $K_d$  of SS in the field in function of  $M/V$  for Cs, Am, Pu and Sr

Table 3 presents the values obtained for  $a$  and  $b$  and specifies the coefficients of determination,  $R^2$  and the p-value of the parameter  $b$  of each fit.

**Table 3:** Parameters  $a$  and  $b$ , determination coefficients  $R^2$  and p-value of parameter  $b$  of the Equation 3 - (\*) indicates the elements with p-value  $> 0.05$

Element	$a$	$b$ (p-value)	$R^2$	Element	$a$	$b$ (p-value)	$R^2$
Am	$6.09 \times 10^5$	-0.839 ( $1.00 \times 10^{-6}$ )	0.44	Ni	$5.21 \times 10^4$	-0.462 ( $2.30 \times 10^{-3}$ )	0.18
As <sup>(*)</sup>	$4.51 \times 10^4$	-0.254 ( $8.00 \times 10^{-2}$ )	0.07	Pb	$2.00 \times 10^6$	-0.610 ( $3.30 \times 10^{-13}$ )	0.60
B	$2.54 \times 10^4$	-1.368 ( $3.30 \times 10^{-7}$ )	0.75	Po	$1.00 \times 10^6$	-1.290 ( $5.00 \times 10^{-7}$ )	0.97
Ba	$3.37 \times 10^4$	-0.515 ( $1.50 \times 10^{-2}$ )	0.54	Pr	$4.00 \times 10^4$	0.5694 ( $1.70 \times 10^{-2}$ )	0.26
Be <sup>(*)</sup>	$4.49 \times 10^4$	-0.066 ( $4.30 \times 10^{-1}$ )	0.02	Pu	$7.15 \times 10^5$	-0.990 ( $1.25 \times 10^{-6}$ )	0.40
Ca	$8.01 \times 10^3$	-0.838 ( $4.40 \times 10^{-7}$ )	0.73	Ra	$2.25 \times 10^4$	-0.238 ( $2.00 \times 10^{-3}$ )	0.19
Cd	$2.35 \times 10^5$	-0.531 ( $9.35 \times 10^{-8}$ )	0.67	Rb	$7.48 \times 10^4$	-1.104 ( $6.25 \times 10^{-9}$ )	0.84
Ce	$7.85 \times 10^4$	0.320 ( $1.60 \times 10^{-3}$ )	0.34	S	$8.03 \times 10^3$	-0.833 ( $9.70 \times 10^{-6}$ )	0.65
Co	$6.97 \times 10^4$	-0.160 ( $1.20 \times 10^{-2}$ )	0.09	Sb	$2.70 \times 10^4$	-0.374 ( $1.00 \times 10^{-3}$ )	0.25
Cr	$1.18 \times 10^5$	-0.227 ( $1.70 \times 10^{-2}$ )	0.11	Se	$1.52 \times 10^5$	-1.096 ( $8.30 \times 10^{-6}$ )	0.66
Cs	$1.80 \times 10^5$	-0.493 ( $4.10 \times 10^{-6}$ )	0.26	Si	$3.20 \times 10^4$	-0.813 ( $1.00 \times 10^{-4}$ )	0.56
Cu <sup>(*)</sup>	$6.09 \times 10^4$	-0.152 ( $2.00 \times 10^{-1}$ )	0.03	Sn <sup>(*)</sup>	$3.18 \times 10^5$	-0.428 ( $6.20 \times 10^{-2}$ )	0.17
Fe <sup>(*)</sup>	$2.92 \times 10^5$	-0.136 ( $2.00 \times 10^{-1}$ )	0.04	Sr	$1.10 \times 10^4$	-0.587 ( $6.00 \times 10^{-5}$ )	0.36

<b>K</b>	3.60×10 <sup>4</sup>	-1.324 (2.33×10 <sup>-7</sup> )	0.76	<b>Th<sup>(*)</sup></b>	1.41×10 <sup>5</sup>	0.504 (2.11×10 <sup>-1</sup> )	0.13
<b>La</b>	5.06×10 <sup>4</sup>	0.5133 (2.00×10 <sup>-2</sup> )	0.25	<b>Ti</b>	2.94×10 <sup>5</sup>	-0.526 (3.20×10 <sup>-3</sup> )	0.37
<b>Mg</b>	7.08×10 <sup>3</sup>	-0.654 (1.20×10 <sup>-3</sup> )	0.43	<b>U</b>	9.72×10 <sup>4</sup>	-0.783 (5.00×10 <sup>-7</sup> )	0.52
<b>Mn<sup>(*)</sup></b>	1.43×10 <sup>5</sup>	-0.150 (2.22×10 <sup>-1</sup> )	0.02	<b>V</b>	1.44×10 <sup>5</sup>	-0.625 (6.00×10 <sup>-3</sup> )	0.34
<b>Mo</b>	1.14×10 <sup>5</sup>	-1.228 (1.71×10 <sup>-6</sup> )	0.59	<b>Zn</b>	3.91×10 <sup>5</sup>	-0.575 (1.30×10 <sup>-4</sup> )	0.29
<b>Na</b>	3.49×10 <sup>3</sup>	-0.360 (3.30×10 <sup>-2</sup> )	0.22				

The parameter  $b$  is negative for 86.5% of the listed elements and it is positive for only five elements (Ce, Th, La, Pr and Ra). However, the relationship was not significant for As, Be, Cu, Mn, Sn and Th for which the p-value of the parameter  $b$  was greater than to 0.05 and the determination coefficient was lower than 0.2. For B, Ba, Ca, Cd, K, Mo, Pb, Po, Rb, S, Se, Si and U, the sensitivity of the  $K_d$  values in the field to  $[SS]$  explained more than 50% of the dataset variability and  $[SS]$  appeared to be a useful cofactor that significantly reduced the variability of  $K_d$  distributions. The interpretation of these results required consideration of the feature that the  $K_d$  datasets for  $SS$  in the field combined  $K_d$  data associated with both anthropogenic radionuclides and/or natural elements. The interest in data for natural elements is to permit filling of  $K_d$  data gaps for those radionuclides which are poorly characterised or where no data has been identified. However, these data require specific attention because their apparent  $K_d$  values can include the partial contribution of some of the element which is naturally present inside the solid particles. These fractions are never in contact with water and are non-exchangeable which can lead to an overestimation of the  $K_d$  especially when the particle size increases.

To evaluate how our datasets could be impacted by the above effect, we assumed that the theoretical decreasing in  $K_d$  values as a function of particle size is maximal in the case of an anthropogenic element (zero concentration inside the particles) and physically limited by the effect of particle size (Abril and Fraga, 1996). The decrease of the  $K_d$  as a function of the radius  $r$  is faster for anthropogenic nuclides when the concentration of the element inside the particles is negligible. For natural nuclides, this decrease is attenuated when the non-exchangeable concentrations of the elements inside the particles are not negligible. At the limit, for highly soluble natural nuclides, the apparent  $K_d$  can increase as the particles radius increases (Abril and Fraga, 1996). In our  $K_d$  datasets the particle size is not reported but, as stated above, it can be assumed in the field that this parameter is positively correlated to the  $M/V$  ratio. This assumption made it possible to apply this analogy to assess the representativeness of our  $K_d$  datasets for deriving  $K_d$  data for natural elements. We assumed that the  $K_d$  value decreases as the  $M/V$  ratio increases, and that this decrease is more rapid when the non-exchangeable fraction of the element inside the particle is low and/or the element is almost insoluble. It can then be assumed that the  $K_d$  datasets for  $SS$  in the field that are most impacted by the use of natural elements are the datasets associated with the weakest decrease in their  $K_d$  values as the  $M/V$  ratio increases. Considering Equation 3, the rate of this decrease is mainly dependent on parameter  $b$  and it can be assumed that the lower this parameter, the less the dataset is affected by the use of data for natural elements. This is consistent with Figure 5 which shows that the correlations between Equation 3 and the datasets increase when the values of parameter  $b$  decrease.

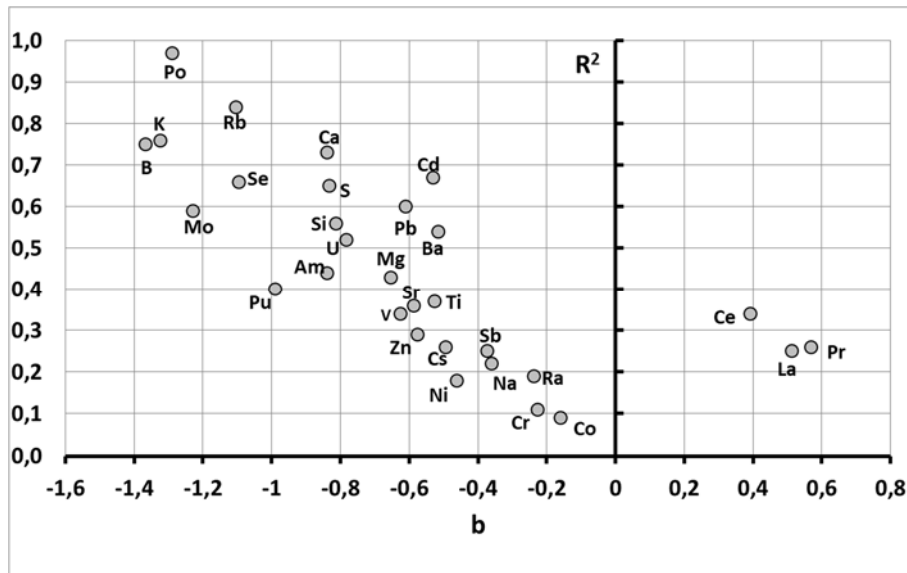


**Figure 5:** Determination coefficients of Equation 3 in function of  $b$

Figure 5 identifies four groups of  $K_d$  datasets.

- Field[1]:  $b < -0.8$

The elements in group [1] are Am, B, Ca, K, Mo, Po, Pu, Rb, S, Se, Si and U. They were characterized by a low  $b$  value and determination coefficients greater than 0.4. It can be assumed that the  $K_d$  datasets of these elements were less affected by the use of  $K_d$  data for natural elements and that the proposed  $K_d$  distributions could be considered as directly applicable in case of anthropogenic releases. In Table 2, the  $K_d$  distributions of these elements for  $SS$  in the field are labelled Field[1].

- Field[2]:  $-0.8 < b < -0.4$  and  $R^2 > 0.2$

The elements in group [2] are Ba, Cd, Cs, Mg, Pb, Sr, Ti, V and Zn. The  $K_d$  datasets of these elements for  $SS$  in the field can be potentially affected by the use of natural elements. Thus, applying these distributions for anthropogenic releases could lead to an overestimation of the  $K_d$  values. In Table 2, the  $K_d$  distributions of these elements for  $SS$  in the field are labelled Field[2].

- Field[3]:  $-0.4 < b < 0$  or  $R^2 < 0.2$

The elements in group [3] are Co, Cr, Na, Ni, Ra and Sb. The  $K_d$  datasets for  $SS$  in the field of these elements could be significantly impacted by the use of natural elements. In Table 2, the  $K_d$  distributions of these elements for  $SS$  in the field are labelled Field[3].

- Field[4]:  $0 < b$

The elements in group [4] are Ce, La and Pr. The  $K_d$  datasets of these elements showed an increase in the  $K_d$  values when the  $M/V$  ratio increased which is typical of the behavior of natural soluble elements under environmental conditions. Consequently, the  $K_d$  distributions presented in Table 2 for the elements of group [4] were representative of environmental conditions and could not be directly applied for a scenario of anthropogenic releases without

explicit acceptance that there was probably an overestimation of the  $K_d$ . In Table 2, the  $K_d$  distributions of these elements for  $SS$  in the field are labelled Field[4].

- Field[0]

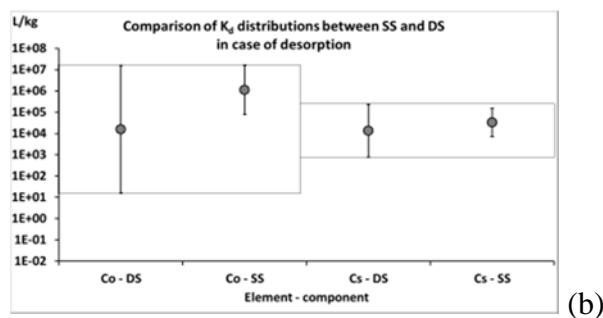
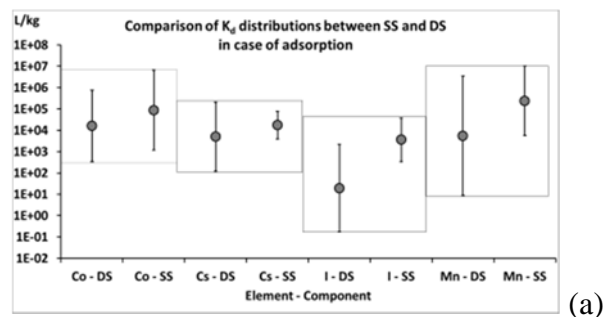
This applies to  $K_d$  datasets for  $SS$  in the field which are not adequately characterised to apply this approach (Cm, I, Ru) or for which the fit of the Equation 3 is not significant (As, Be, Cu, Mn, Sn and Th). Therefore, they were not interpreted and labelled Field[0] in Table 2.

#### 4.2. INTERPRETATION OF THE $K_d$ DISTRIBUTIONS FOR DS IN THE FIELD BY COMPARISONS WITH DISTRIBUTIONS FOR SS IN THE FIELD

We initially hypothesised that the  $K_d$  values are greater for  $SS$  than for  $DS$ . By calculating separate  $K_d$  distributions for  $SS$  and  $DS$  we were able to test this hypothesis. The  $K_d$  distributions of these two components were compared when they were available for the same exchange conditions. The testable combinations were:

1. Co, Cs, I and Mn for adsorption,
2. Co and Cs for desorption
3. As, Cd, Co, Cr, Cs, Cu, Fe, La, Mn, Ni, Pb, Po, Ra, U and Zn for field conditions.

For each exchange condition, Figure 6 shows the  $K_d$  distributions for  $SS$  and  $DS$  and Figure 7 presents the ratios between the  $GSD$  values for  $SS$  and  $DS$ .



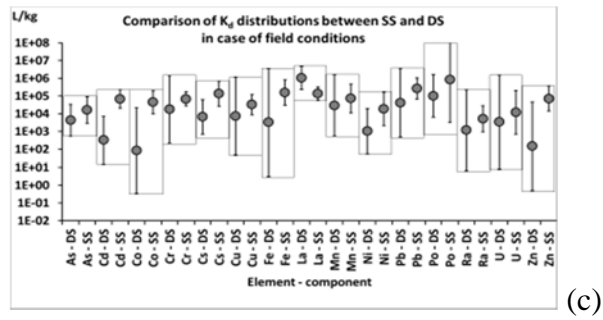


**Figure 6:**  $K_d$  distributions for *SS* and *DS* in the case of adsorption (a), desorption (b) and field conditions (c) (the point corresponds to the *GM* and the upper and lower error bars correspond to 5 and 95 percentiles respectively)

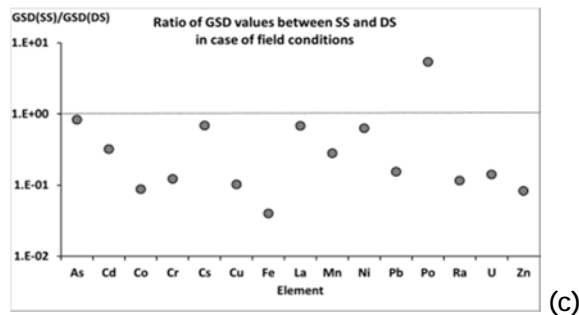
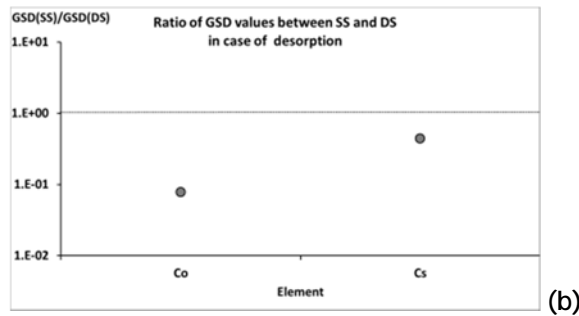
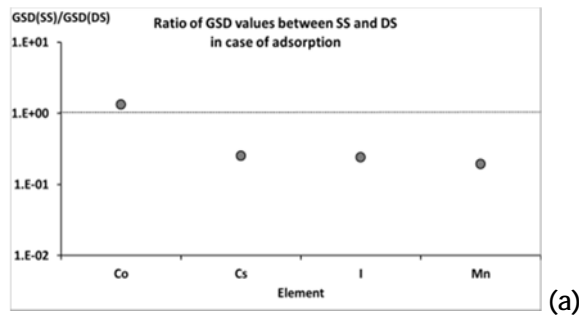


**Figure 7:** Ratio of *GSD* values between *SS* and *DS* in the case of adsorption (a), desorption (b) and field conditions (c)

In Figure 6a, the adsorption  $K_d$  distributions of Co, I and Mn were significantly higher for *SS* than for *DS* and overlapped for Cs. In the case of desorption (Figure 6b), the  $K_d$  distributions of *SS* and *DS* overlapped for Co and Cs. In Figure 6c, under field conditions, the  $K_d$  distributions for *SS* were higher than those of *DS* for As, Cd, Cs, Ni and Zn and overlapped for Cr, Cu, Fe, Mn, Pb, Po, Ra and U. For La, the  $K_d$  distribution under field conditions was

greater for *DS* than for *SS*. The mean value of the ratios between the GM values for *SS* and *DS* was 80 and ranged from 1 to 1000 with the exception of La in the field for which the ratio was significantly lower than 1. Under field conditions, this ratio ranged from 1 to 10 for most elements (As, Cr, Cu, Mn, Pb, Po, Ra, U), from 10 to 100 for Cs, Fe and Ni and exceeded 100 for Cd, Co and Zn.

In Figures 7a,b,c, the ratios of GSD values for *SS* and *DS* are shown. All the ratios were lower than 1 with the exception of Co (adsorption) and Po (under field conditions). The mean ratio value of 0.6 showed that the  $K_d$  distributions for *SS* were less variable than the  $K_d$  distributions for *DS*. This was an expected outcome because of the differences between the contamination kinetics and the particles sizes of *DS* and *SS*. The contamination kinetic of *DS* was more variable than that of *SS* because it is affected by the kinetics of adsorption/desorption and also by the sedimentation rate of suspended particles. Consequently, equilibrium conditions were more infrequent for *DS* than for *SS*, which increased the variability of the  $K_d$  values measured for *DS*. Conversely, the variability and ranges of the particle size distributions were larger for *DS* than for *SS*, which also contributed to increasing the variability of  $K_d$  distribution for *DS*.

These comparisons highlighted the benefit of separately considering  $K_d$  distributions of *DS* and *SS* because the  $K_d$  values were significantly higher for *SS* than for *DS* and the variability of the distributions was higher for *DS* than for *SS*. Using this approach, the distinction between *DS* and *SS* allowed the derivation of more realistic  $K_d$  values for each compartment and reduced the variability of their  $K_d$  distributions. However, as for  $K_d$  of *SS* in the field, the use of  $K_d$  data including data of natural elements for *DS* in the field required an assessment of the representativeness of these  $K_d$  datasets. Continuing the approach applied to *SS* (see 4.1), this assessment was based on the ratio between the GM of  $K_d$  for *DS* in the field with the value given by Equation 2 where the  $M/V$  ratio of superficial sediments was assumed to be close to 650 g/L, which corresponds to a mean porosity of 0.75. Assuming a link of decreasing  $K_d$  values when the  $M/V$  ratio increases, it was considered that the representativeness of the  $K_d$  dataset for *DS* in the field was identical to that of the  $K_d$  dataset for *SS* in the field when this ratio was lower than or equal to 10. A ratio greater than 10 indicated a significant increase in the  $K_d$  value when the  $M/V$  ratio increased and suggested the need to consider a classification with one step higher than that used for the  $K_d$  dataset for *SS* in the field.

The approach was only applied to elements for which the dataset allowed determination of statistical distributions for both *SS* and *DS* in the field (Figure 8): As, Cd, Co, Cr, Cs, Cu, Fe, La, Mn, Ni, Pb, Po, Ra, U, Zn. The method could not be applied to elements (Ag, Ba, Ca, Mg, Mo, Sb, Se, Sr, Th, Ti and V) which reported both *SS* and *DS* field  $K_d$ , where one or both had a classification of Field[0] in Table 2.

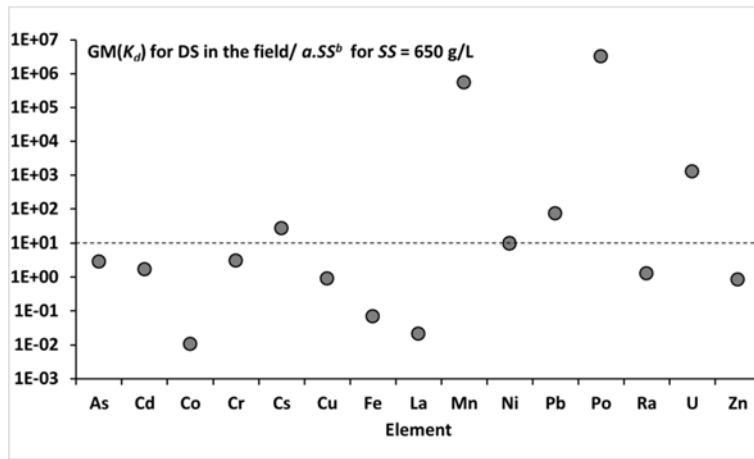


**Figure 8:**  $GM(K_d)$  for  $DS$  in the field divided by  $a.SS^b$  for  $SS = 650$  g/L

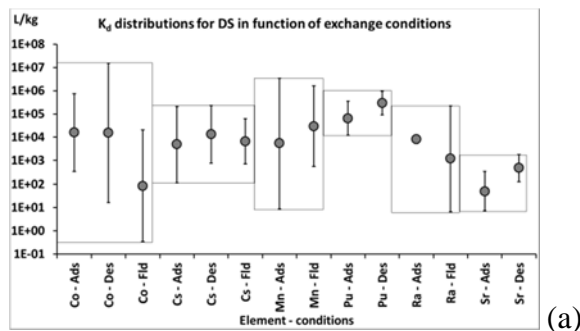
The ratio was lower than 10 for As, Cd, Co, Cr, Cu, Fe, La, Ni, Ra and Zn. For these elements, the representativeness of the  $K_d$  datasets for  $DS$  in the field was classified at the same level as that for their  $K_d$  dataset for  $SS$  in the field.

The ratio was significantly greater than 10 for Cs, Mn, Pb, Po and U. The representativeness of the  $K_d$  datasets of these elements for  $DS$  in the field was ranked one level higher than their  $K_d$  datasets for  $SS$  in the field.

The  $K_d$  datasets for  $DS$  in the field for Dy, Er, Eu, Gd, Hf, Ho and Li were obtained only for natural conditions and they cannot be compared to  $K_d$  datasets for  $SS$  in the field. Consequently, and by default, their datasets are classified Field[3].

#### 4.3. COMPARISON OF $K_d$ DISTRIBUTIONS AS A FUNCTION OF EXCHANGE CONDITIONS

This third analysis compared the  $K_d$  distributions of  $DS$  and  $SS$  as a function of the exchange conditions. For  $DS$  (Figure 9a), the dataset was sufficiently large to allow such comparisons for Co (adsorption, desorption, field), Cs (adsorption, desorption, field), Mn (adsorption, field), Pu (adsorption, desorption), Ra (adsorption, field) and Sr (adsorption, desorption). For  $SS$  (Figure 9b), comparisons were possible for Ag (adsorption, desorption), Ba (adsorption, field), Co (adsorption, desorption, field), Cs (adsorption, desorption, field), I (adsorption, field), Mn (adsorption, desorption, field), Sb (adsorption, field) and Sr (adsorption, field).



(a)

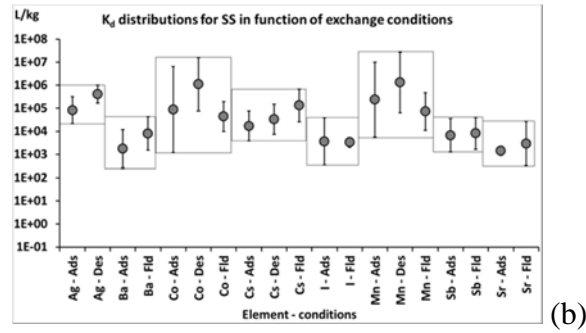


**Figure 9:**  $K_d$  distributions of *DS* (a) and *SS* (b) as a function of exchange conditions (points correspond to *GM* and high and low levels correspond respectively to 5 and 95 percentiles)

Whatever the component and element, desorption  $K_d$  distributions all had higher *GM* values compared with adsorption  $K_d$  distributions. For *DS*, distributions for Pu and Sr were higher for desorption than for adsorption and they overlapped for Co, Cs and Ra. For *SS*, distributions for desorption were higher than for adsorption for all the reported elements (Ag, Co, Cs and Mn).

For field conditions,  $K_d$  distributions were similar to those of other exchange conditions with the exception of Co for *DS* and Cs for *SS* for which the distributions in the field were respectively lower and higher than the other exchange conditions.

From a statistical point of view, the comparison of the  $K_d$  distributions as a function of exchange conditions showed that it is not useful to consider separate  $K_d$  distributions for adsorption and desorption because these distributions overlap in many cases. Nevertheless, the analysis has shown that the *GM* values are systematically greater in the case of desorption. In practice, the comparison suggested that specific desorption or adsorption  $K_d$  would be preferred data to use for deterministic calculations. For probabilistic calculations, the difference between the  $K_d$  distributions as a function of the exchange conditions will be less obvious.

## 5. CONCLUSIONS

- Comparisons between  $K_d$  distributions of suspended and deposited sediments showed that the  $K_d$  values were significantly higher for suspended than for deposited sediments and that the variability was higher for deposited than for suspended sediments. In practice, the separation of these two components enabled more realistic  $K_d$  values to be derived and also reduced the variability of the  $K_d$  distributions.
- In the field, the variability of  $K_d$  distributions for suspended sediments can be significantly reduced as a function of the suspended load. For suspended sediments in the field, this parameter explained more than 50% of the variability of the  $K_d$  datasets of U, Si, Mo, Pb, S, Se, Cd, Ca, B, K, Ra and Po.
- Analysis of  $K_d$  distributions as a function of exchange conditions showed that geometric means were systematically greater for desorption than for adsorption while distributions generally overlapped. If it is clearly relevant to distinguish specific  $K_d$  values as a function of exchange conditions in case of deterministic calculations, but not for probabilistic calculations.

The possible combinations between the 49 elements, the two components and the three conditions gave a total of 294 distributions. Currently, 63% of these combinations are associated to only one publication or expert judgement, 7% are associated to a mean value and 30% are associated to a log-normal distribution. Consequently, more work is needed to fully characterise these distributions. This task is continuing during the current IAEA program, MODARIA II, where the priority is being given to the gaps identified as the most critical in terms of the different radiological impact scenarios to the environment and human populations.

## **6. ACKNOWLEDGEMENTS**

The present work was carried out in the framework of MODARIA (Modelling and Data for Radiological Impact Assessments) programme of the International Atomic Energy Agency. The authors would like to express their sincere thanks to P. Ciffroy which kindly supplied the dataset used to determine  $K_d$  distributions published in TRS 472 (IAEA, 2010). Our thanks are also addressed to M. Vidal and D. Kaplan for their contributions and their scientific support during the MODARIA program. The EC project STAR funded placements of C. Wells at IRSN during part of this study.

## REFERENCES

- Abril, J.M. and Fraga, E. (1996). Some physical and chemical features of the variability of Kd distributions coefficients for radionuclides J. Environ. Radioact., **30**, 253-270.
- Allison, J.D. and Allison, T.L. (2005). Partition coefficient for metals in surface water, soil, and waste. EPA/600/R-05/074 Washington, DC, United States.
- Benoit, G., Oktay-Marshall, S.D., Cantu, A., II, Hood, E.M., Coleman, C.H., Corapcioglu, M.O., and Santschi, P.H. (1994). Partitioning of Cu, Pb, Ag, Zn, Fe, Al, and Mn between filter-retained particles, colloids, and solution in six Texas estuaries. Mar. Chem., **45**, 307-336.
- Benoit, G. and Rozan, T.F. (1999). The influence of size distribution on the particle concentration effect and trace metal partitioning in rivers. Geochimica and Cosmochimica Acta, **63**, 1, 113-127.
- BIOMOVS (1990). On the validity of environmental transfer models. In: Proceedings of a Symposium, Stockholm, Sweden. Sundt Artprint, Stockholm, Sweden, ISBN 91-630-0437-2 (Swedish Radiation Protection Institute).
- Boudreau, P.B. (1997). Diagenetic models and their implementation. Modelling transport and reactions in aquatic sediments. Springer, 414pp.
- Brown, J.E., Alfonso, B., Avila, R., Beresford, N.A., Copplestone, D., Pröhl, G. and Ulanovsky, A. (2008). The ERICA Tool. J. Environ. Radioact., **99**, 1371-1383.
- Ciffroy, P., Durrieu, G. and Garnier, J-M. (2009). Probabilistic distribution coefficients (Kds) in freshwater for radioisotopes of Ag, Am, Ba, Be, Ce, Co, Cs, I, Mn, Pu Ra, Ru, Sb, Sr and Th. – Implications for uncertainty analysis of models simulating the transport of radionuclides in rivers, J. Environ. Radioact., **100**, 9, 785-794.
- Durrieu, G., Ciffroy, P. and Garnier, J.M. (2006). A weighted bootstrap method for the determination of probability density functions of freshwater distribution coefficients (Kds) of Co, Cs, Sr and I radioisotopes. Chemosphere, **65**, 8, 1308-1320.
- Duchesne, S., Boyer, P. and Beaugelin-Seiller, K. (2003). Sensitivity and uncertainty analysis of a model computing radionuclides transfers in fluvial ecosystems (CASTEAUR): application to <sup>137</sup>Cs accumulation in chubs. Ecological Modelling, **166**, 257-276.
- Eguchi, S. (2017). Behaviour of radioactive cesium in agricultural environment. Journal of Japanese Society of Soil Physics, **135**, 9-23.
- Eyrolle-Boyer, F., Boyer, P., Garcia-Sanchez, L., Metivier, J.M., Onda, Y., De Vismes, A., Cagnat, X., Boulet, B. and Cossonnet, C. (2016). Behaviour of radiocaesium in coastal rivers of the Fukushima Prefecture (Japan) during conditions of low flow and low turbidity - Insight on the possible role of small particles and detrital organic compounds. J. Environ. Radioact., **151**, 328-340.
- Francis, C.W. and Brinkley, F.S. (1976). Preferential adsorption of <sup>137</sup>Cs to micaceous minerals in contaminated freshwater sediment. Nature, **260**, 511-513.

Garcia-Sanchez, L., Loffredo, N., Mounier, S., Martin-Garin, A. and Coppin, F. (2014). Kinetics of selenate sorption in soil as influenced by biotic and abiotic conditions: a stirred flow-through reactor study. *J. Environ. Radioact.*, **138**, 38-49.

Goldberg, S., Criscenti, L.J., Turner, D.R. and Davis, J.A. and Cantrell, K.J. (2007). Adsorption – desorption processes in subsurface reactive transport modeling. *Vadose Zone J.*, **6**, 407-435.

Gonze, M.A., Mourlon, C., Garcia-Sanchez, L., Le Dizes, S., Nicoulaud, V., Gerber, P.P. and Vermorel, F. (2011). SYMBIOSE: a simulation platform for conducting radiological risk assessments. International Conference on Radioecology and Environmental Radioactivity (ICRER). 19-24 June 2011, Hamilton, Ontario, Canada.

He, Q. and Walling D.E. (1996). Interpreting particle size effects in the adsorption of  $^{137}\text{Cs}$  and unsupported  $^{210}\text{Pb}$  by mineral soils and sediments. *J. Environ. Radioact.*, **30**, 117-137.

Honeyman, B.D. and Santschi, P.H. (1988). Metals in aquatic systems. *Environ. Sci. Technol.*, **22**, 862–871.

IAEA (1994). Handbook of Parameter Values for the Prediction of Radionuclide Transfer in Temperate Environments. Technical Report Series, IAEA-TRS 364, IAEA, Vienna.

IAEA (2000). Modelling of the transfer of radiocaesium from deposition to lake ecosystems. IAEA-TECDOC 1143, IAEA, Vienna, Austria.

IAEA (2001). Generic Models for use in Assessing the impact of discharges of radioactive substances to the environment. Safety Report Series, IAEA-SRS 19, IAEA, Vienna.

IAEA (2010). Handbook of Parameter Values for the Prediction of Radionuclide Transfer in Terrestrial and Freshwater Environments. Technical Reports Series, IAEA-TRS 472, IAEA, Vienna.

IAEA (2012). A summary report of the results of the EMRAS programme (2003–2007). IAEA-TECDOC 1678, IAEA, Vienna.

Kabata-Pendias, A. (2010). Trace Elements in Soils and Plants. CRC Press, Boca Raton, FL, 377 pp.

Kaplan, D.I. (2016). Geochemical Data Package for Performance Assessment and Composite Analysis at the Savannah River Site - Supplemental Radionuclides. SRNL-STI-2016-00267, Rev 0, Savannah River National Laboratory, Aiken, SC.

Mehta, A.J. (2014). An introduction to hydraulics of fine sediment transport. New Jersey World Scientific, Advanced Series on Ocean Engineering, **38**, 1039 pp.

Morse, J.W. and Arakaki, T. (1993). Adsorption and coprecipitation of divalent metals with mackinawite (FES), *Geochim. Cosmochim.*, **57**, 3635-3640.

Müller, G. and Förstner, U. (1968). General relationship between suspended sediment concentration and water discharge in the Alpenrhein and other rivers. *Nature*, **217**, 244-245.

Neal, C., Robson, A.J., Jeffery, H.A., Harrow, M.L., Neal, M., Smith, C.J. and Jarvie, H.P. (1997). Trace element inter-relationships for the Humber rivers: inferences for hydrological and chemical controls. *The Science of the Total Environment*, **194-195**, 321-343.

Neal, C. (2007). Rare earth element concentrations in dissolved and acid available particulate forms for eastern UK rivers. *Hydrol. Earth Syst. Sci.*, **11(1)**, 313-327.

Neal, C., Rowland, P., Scholefield, P., Vincent, C., Woods, C. and Sleep, D. (2011). The Ribble/Wyre observatory: Major, minor and trace elements in rivers draining from rural headwaters to the heartlands of the NW England historic industrial base. *Science of the Total Environment*, **409**, 1516–1529.

Onishi, Y., Serne, R.J., Arnold, E.M., Cowen, C.E. and Thompson, F.L. (1991). Critical review: Radionuclide transport, sediment transport, and water quality mathematical modelling and radionuclide adsorption/desorption mechanisms. Rep. NUREG/CR-1322, PNL-2901, Pacific Northwest Lab., Richmond, WA.

Rivera, N., Choi, S., Strepka, C., Mueller, K., Perdrial, N., Chorover, J. and O'Day, P.A. (2011). Cesium and strontium incorporation into zeolite-type phases during homogeneous nucleation from caustic solutions, *Am. Mineralogist*, **96**, 1809-1820.

Sheppard, S., Long, J., Sanipelli, B. and Sohlenius, G. (2009). Solid/liquid Partition coefficients (Kd) for selected soils and sediments at Forsmark and Laxemar-Simpevarp. R-09-27, Swedish Nuclear Fuel and Waste Management Co., Stockholm.

Sheppard, S.C. (2011). Robust prediction of Kd from soil properties for environmental assessment. *Human and Ecological Risk Assessment*, **17**, 263-279.

Sigg, L., Behra, P. and Stumm, W. (2000). *Chimie des milieux aquatiques*. Third Edition, Dunod, Paris, 567 pp.

Simon-Cornu, M., Beaugelin-Seiller, K., Boyer, P., Calmon, P., Garcia-Sanchez, L., Murlon, C., Nicoulaud, V., Sya, M. and Gonze, M.A. (2015) Evaluating variability and uncertainty in radiological impact assessment using SYMBIOSE. *J. Environ. Radioact.*, **139**, 91–102.

Sparks, D.L. (2003). *Environmental Soil Chemistry*. Academic Press, New York, 448 pp.

Sposito, G. (2008). *The Chemistry of Soils*. Oxford University Press, New York.

Stumm, W. and Morgan, J.J. (2012). *Aquatic Chemistry, Chemical Equilibria and Rates in Natural Waters*. John Wiley & Sons, Inc., New York.

Tesorio, A. and Pankow, J.F. (1996). Solid solution partitioning of Sr<sup>2+</sup>, Ba<sup>2+</sup>, and Cd<sup>2+</sup> to calcite. *Geochim. Cosmochim. Acta*, **60**, 1053-1063.

Thibault, D.H., Sheppard, M.I. and Smith, P.A. (1990). A critical compilation and review of default soil solid/liquid partition coefficients, Kd, for use in environmental assessments. AECL 10125, Atomic Energy of Canada Limited, Pinawa, Manitoba, Canada.

Walling, D.E., Owens, P.N., Waterfall, B.D., Leeks, G.J.L and Wass, P.D. (2000). The particle size characteristics of fluvial suspended sediment in the Humber and Tweed catchments, UK. *The Science of the Total Environment*. **251/252**, 205-222.

Xu, C., Athon, M., Ho, Y.F., Chang, H.S., Zhang, S., Kaplan, D.I., Schwehr, K.A., DiDonato, N., Hatcher, P.G. and Santschi, P.H. (2014). Plutonium immobilization and re-mobilization by soil mineral and organic matter in the far-field of the Savannah River Site, USA. *Environ. Sci. Technol.*, **48**, 3186-3195.

## ANNEXE I - METHOD TO DETERMINE LOG-NORMAL DISTRIBUTIONS

The empirical CDF is obtained by classifying the  $K_d$  values in the ascending order and by determining  $f(K_{d_i})$ , the occurrence frequency of each value  $K_{d_i}$ .

$$f(K_{d_i}) = n(K_{d_i})/N$$

Where  $n(K_{d_i})$  is the occurrence of the  $K_{d_i}$  value and  $N$  is the number of individual of the dataset.

The empirical CDF is then given by:

$$CDF(K_{d_i}) = CDF(K_{d_{i-1}}) + f(K_{d_i}) \text{ with } CDF(K_{d_0}) = f(K_{d_0})$$

The log-normal CDF corresponds to the following relationship:

$$CDF^*(K_{d_i}) = \frac{1}{2} + \frac{1}{2} \cdot erf\left(\frac{\log(K_{d_i}) - \mu}{\sigma \cdot \sqrt{2}}\right)$$

Where  $\mu = \sum f(K_{d_i}) \cdot \log(K_{d_i})$  is the arithmetic mean of  $\log(K_d)$ ,  $\sigma = \sqrt{\sum f(K_{d_i}) \cdot (\log(K_{d_i}) - \mu)^2}$  is the standard deviation of  $\log(K_d)$  and  $erf$  is the error function.

$\mu$  and  $\sigma$  are obtained by fitting CDF with CDF\* with the least squares method and GM and GSD are given by:

$$GM = \text{antilog}(\mu)$$

$$GSD = \text{antilog}(\sigma)$$

The fit between CDF and CDF\* is evaluated using the Kolmogorov-Smirnov test (KS-test) which compares the maximal disparity between CDF and CDF\* to the maximal value given by the Kolmogorov table as a function of quantiles and number of individual. Here, the fit is assumed valid if the maximal disparity between CDF and CDF\* is lower than the value given by this table for the same number of individual and a quantile of 0.95.

## REFERENCES

- Abril, J.M. and Fraga, E. (1996). Some physical and chemical features of the variability of Kd distributions coefficients for radionuclides J. Environ. Radioact., **30**, 253-270.
- Allison, J.D. and Allison, T.L. (2005). Partition coefficient for metals in surface water, soil, and waste. EPA/600/R-05/074 Washington, DC, United States.
- Benoit, G., Oktay-Marshall, S.D., Cantu, A., II, Hood, E.M., Coleman, C.H., Corapcioglu, M.O., and Santschi, P.H. (1994). Partitioning of Cu, Pb, Ag, Zn, Fe, Al, and Mn between filter-retained particles, colloids, and solution in six Texas estuaries. Mar. Chem., **45**, 307-336.
- Benoit, G. and Rozan, T.F. (1999). The influence of size distribution on the particle concentration effect and trace metal partitioning in rivers. Geochimica and Cosmochimica Acta, **63**, 1, 113-127.
- BIOMOVS (1990). On the validity of environmental transfer models. In: Proceedings of a Symposium, Stockholm, Sweden. Sundt Artprint, Stockholm, Sweden, ISBN 91-630-0437-2 (Swedish Radiation Protection Institute).
- Boudreau, P.B. (1997). Diagenetic models and their implementation. Modelling transport and reactions in aquatic sediments. Springer, 414pp.
- Brown, J.E., Alfonso, B., Avila, R., Beresford, N.A., Copplestone, D., Pröhl, G. and Ulanovsky, A. (2008). The ERICA Tool. J. Environ. Radioact., **99**, 1371-1383.
- Ciffroy, P., Durrieu, G. and Garnier, J-M. (2009). Probabilistic distribution coefficients (Kds) in freshwater for radioisotopes of Ag, Am, Ba, Be, Ce, Co, Cs, I, Mn, Pu Ra, Ru, Sb, Sr and Th. – Implications for uncertainty analysis of models simulating the transport of radionuclides in rivers, J. Environ. Radioact., **100**, 9, 785-794.
- Durrieu, G., Ciffroy, P. and Garnier, J.M. (2006). A weighted bootstrap method for the determination of probability density functions of freshwater distribution coefficients (Kds) of Co, Cs, Sr and I radioisotopes. Chemosphere, **65**, 8, 1308-1320.
- Duchesne, S., Boyer, P. and Beaugelin-Seiller, K. (2003). Sensitivity and uncertainty analysis of a model computing radionuclides transfers in fluvial ecosystems (CASTEAUR): application to <sup>137</sup>Cs accumulation in chubs. Ecological Modelling, **166**, 257-276.
- Eguchi, S. (2017). Behaviour of radioactive cesium in agricultural environment. Journal of Japanese Society of Soil Physics, **135**, 9-23.
- Eyrolle-Boyer, F., Boyer, P., Garcia-Sanchez, L., Metivier, J.M., Onda, Y., De Vismes, A., Cagnat, X., Boulet, B. and Cossonnet, C. (2016). Behaviour of radiocaesium in coastal rivers of the Fukushima Prefecture (Japan) during conditions of low flow and low turbidity - Insight on the possible role of small particles and detrital organic compounds. J. Environ. Radioact., **151**, 328-340.
- Francis, C.W. and Brinkley, F.S. (1976). Preferential adsorption of <sup>137</sup>Cs to micaceous minerals in contaminated freshwater sediment. Nature, **260**, 511-513.

Garcia-Sanchez, L., Loffredo, N., Mounier, S., Martin-Garin, A. and Coppin, F. (2014). Kinetics of selenate sorption in soil as influenced by biotic and abiotic conditions: a stirred flow-through reactor study. *J. Environ. Radioact.*, **138**, 38-49.

Goldberg, S., Criscenti, L.J., Turner, D.R. and Davis, J.A. and Cantrell, K.J. (2007). Adsorption – desorption processes in subsurface reactive transport modeling. *Vadose Zone J.*, **6**, 407-435.

Gonze, M.A., Mourlon, C., Garcia-Sanchez, L., Le Dizes, S., Nicoulaud, V., Gerber, P.P. and Vermorel, F. (2011). SYMBIOSE: a simulation platform for conducting radiological risk assessments. International Conference on Radioecology and Environmental Radioactivity (ICRER). 19-24 June 2011, Hamilton, Ontario, Canada.

He, Q. and Walling D.E. (1996). Interpreting particle size effects in the adsorption of  $^{137}\text{Cs}$  and unsupported  $^{210}\text{Pb}$  by mineral soils and sediments. *J. Environ. Radioact.*, **30**, 117-137.

Honeyman, B.D. and Santschi, P.H. (1988). Metals in aquatic systems. *Environ. Sci. Technol.*, **22**, 862–871.

IAEA (1994). Handbook of Parameter Values for the Prediction of Radionuclide Transfer in Temperate Environments. Technical Report Series, IAEA-TRS 364, IAEA, Vienna.

IAEA (2000). Modelling of the transfer of radiocaesium from deposition to lake ecosystems. IAEA-TECDOC 1143, IAEA, Vienna, Austria.

IAEA (2001). Generic Models for use in Assessing the impact of discharges of radioactive substances to the environment. Safety Report Series, IAEA-SRS 19, IAEA, Vienna.

IAEA (2010). Handbook of Parameter Values for the Prediction of Radionuclide Transfer in Terrestrial and Freshwater Environments. Technical Reports Series, IAEA-TRS 472, IAEA, Vienna.

IAEA (2012). A summary report of the results of the EMRAS programme (2003–2007). IAEA-TECDOC 1678, IAEA, Vienna.

Kabata-Pendias, A. (2010). Trace Elements in Soils and Plants. CRC Press, Boca Raton, FL, 377 pp.

Kaplan, D.I. (2016). Geochemical Data Package for Performance Assessment and Composite Analysis at the Savannah River Site - Supplemental Radionuclides. SRNL-STI-2016-00267, Rev 0, Savannah River National Laboratory, Aiken, SC.

Mehta, A.J. (2014). An introduction to hydraulics of fine sediment transport. New Jersey World Scientific, Advanced Series on Ocean Engineering, **38**, 1039 pp.

Morse, J.W. and Arakaki, T. (1993). Adsorption and coprecipitation of divalent metals with mackinawite (FES), *Geochim. Cosmochim.*, **57**, 3635-3640.

Müller, G. and Förstner, U. (1968). General relationship between suspended sediment concentration and water discharge in the Alpenrhein and other rivers. *Nature*, **217**, 244-245.

Neal, C., Robson, A.J., Jeffery, H.A., Harrow, M.L., Neal, M., Smith, C.J. and Jarvie, H.P. (1997). Trace element inter-relationships for the Humber rivers: inferences for hydrological and chemical controls. *The Science of the Total Environment*, **194-195**, 321-343.

Neal, C. (2007). Rare earth element concentrations in dissolved and acid available particulate forms for eastern UK rivers. *Hydrol. Earth Syst. Sci.*, **11(1)**, 313-327.

Neal, C., Rowland, P., Scholefield, P., Vincent, C., Woods, C. and Sleep, D. (2011). The Ribble/Wyre observatory: Major, minor and trace elements in rivers draining from rural headwaters to the heartlands of the NW England historic industrial base. *Science of the Total Environment*, **409**, 1516–1529.

Onishi, Y., Serne, R.J., Arnold, E.M., Cowen, C.E. and Thompson, F.L. (1991). Critical review: Radionuclide transport, sediment transport, and water quality mathematical modelling and radionuclide adsorption/desorption mechanisms. Rep. NUREG/CR-1322, PNL-2901, Pacific Northwest Lab., Richmond, WA.

Rivera, N., Choi, S., Strepka, C., Mueller, K., Perdrial, N., Chorover, J. and O'Day, P.A. (2011). Cesium and strontium incorporation into zeolite-type phases during homogeneous nucleation from caustic solutions, *Am. Mineralogist*, **96**, 1809-1820.

Sheppard, S., Long, J., Sanipelli, B. and Sohlenius, G. (2009). Solid/liquid Partition coefficients (Kd) for selected soils and sediments at Forsmark and Laxemar-Simpevarp. R-09-27, Swedish Nuclear Fuel and Waste Management Co., Stockholm.

Sheppard, S.C. (2011). Robust prediction of Kd from soil properties for environmental assessment. *Human and Ecological Risk Assessment*, **17**, 263-279.

Sigg, L., Behra, P. and Stumm, W. (2000). *Chimie des milieux aquatiques*. Third Edition, Dunod, Paris, 567 pp.

Simon-Cornu, M., Beaugelin-Seiller, K., Boyer, P., Calmon, P., Garcia-Sanchez, L., Mourlon, C., Nicoulaud, V., Sya, M. and Gonze, M.A. (2015) Evaluating variability and uncertainty in radiological impact assessment using SYMBIOSE. *J. Environ. Radioact.*, **139**, 91–102.

Sparks, D.L. (2003). *Environmental Soil Chemistry*. Academic Press, New York, 448 pp.

Sposito, G. (2008). *The Chemistry of Soils*. Oxford University Press, New York.

Stumm, W. and Morgan, J.J. (2012). *Aquatic Chemistry, Chemical Equilibria and Rates in Natural Waters*. John Wiley & Sons, Inc., New York.

Tesorio, A. and Pankow, J.F. (1996). Solid solution partitioning of Sr<sup>2+</sup>, Ba<sup>2+</sup>, and Cd<sup>2+</sup> to calcite. *Geochim. Cosmochim. Acta*, **60**, 1053-1063.

Thibault, D.H., Sheppard, M.I. and Smith, P.A. (1990). A critical compilation and review of default soil solid/liquid partition coefficients, Kd, for use in environmental assessments. AECL 10125, Atomic Energy of Canada Limited, Pinawa, Manitoba, Canada.

Walling, D.E., Owens, P.N., Waterfall, B.D., Leeks, G.J.L and Wass, P.D. (2000). The particle size characteristics of fluvial suspended sediment in the Humber and Tweed catchments, UK. *The Science of the Total Environment*. **251/252**, 205-222.

Xu, C., Athon, M., Ho, Y.F., Chang, H.S., Zhang, S., Kaplan, D.I., Schwehr, K.A., DiDonato, N., Hatcher, P.G. and Santschi, P.H. (2014). Plutonium immobilization and re-mobilization by soil mineral and organic matter in the far-field of the Savannah River Site, USA. *Environ. Sci. Technol.*, **48**, 3186-3195.

## ANNEXE I - METHOD TO DETERMINE LOG-NORMAL DISTRIBUTIONS

The empirical CDF is obtained by classifying the  $K_d$  values in the ascending order and by determining  $f(K_{d_i})$ , the occurrence frequency of each value  $K_{d_i}$ .

$$f(K_{d_i}) = n(K_{d_i})/N$$

Where  $n(K_{d_i})$  is the occurrence of the  $K_{d_i}$  value and  $N$  is the number of individual of the dataset.

The empirical CDF is then given by:

$$CDF(K_{d_i}) = CDF(K_{d_{i-1}}) + f(K_{d_i}) \text{ with } CDF(K_{d_0}) = f(K_{d_0})$$

The log-normal CDF corresponds to the following relationship:

$$CDF^*(K_{d_i}) = \frac{1}{2} + \frac{1}{2} \cdot erf\left(\frac{\log(K_{d_i}) - \mu}{\sigma \cdot \sqrt{2}}\right)$$

Where  $\mu = \sum f(K_{d_i}) \cdot \log(K_{d_i})$  is the arithmetic mean of  $\log(K_d)$ ,  $\sigma = \sqrt{\sum f(K_{d_i}) \cdot (\log(K_{d_i}) - \mu)^2}$  is the standard deviation of  $\log(K_d)$  and  $erf$  is the error function.

$\mu$  and  $\sigma$  are obtained by fitting CDF with CDF\* with the least squares method and GM and GSD are given by:

$$GM = \text{antilog}(\mu)$$

$$GSD = \text{antilog}(\sigma)$$

The fit between CDF and CDF\* is evaluated using the Kolmogorov-Smirnov test (KS-test) which compares the maximal disparity between CDF and CDF\* to the maximal value given by the Kolmogorov table as a function of quantiles and number of individual. Here, the fit is assumed valid if the maximal disparity between CDF and CDF\* is lower than the value given by this table for the same number of individual and a quantile of 0.95.

## List of tables

**Table 1:** List of elements used in ERICA tool and SYMBIOSE platform based upon the quality criteria of available  $K_d$  values

**Table 2:**  $K_d$  distributions in function of environmental components ( $SS$  and  $DS$ ) and conditions of liquid-solid exchange (adsorption, desorption, field)

**Table 3:** Parameters  $a$  and  $b$ , determination coefficients  $R^2$  and p-value of parameter  $b$  of the Equation 3 - (\*) indicates the elements with p-value  $> 0.05$

**Table 3:** List of elements used in ERICA tool and SYMBIOSE platform based upon the quality criteria of available  $K_d$  values

Element	Quality criteria	Element	Quality criteria	Element	Quality criteria
Ac	0	Fr	1	Pu	3
Ag	3	Gd	0	Ra	3
Am	3	H	1	Rb	0
As	1	Hg	1	Rh	1
At	1	I	3	Rn	0
Au	0	In	1	Ru	3
Ba	3	Ir	0	S	1
Be	3	La	0	Sb	3
Bi	1	Mn	3	Se	1
Br	0	Mo	1	SS	1
C	1	Na	1	Sn	1
Ca	1	Nb	1	Sr	3
Cd	0	Nd	0	Tc	1
Ce	3	Ni	1	Te	1
Cf	0	Np	2	Th	3
Cl	1	P	0	Tl	1
Cm	2	Pa	0	U	2
Co	3	Pb	1	W	0
Cr	1	Pd	0	Y	1
Cs	3	Pm	2	Zn	2
Eu	2	Po	1	Zr	2
Fe	2	Pr	1		

**Table 4:**  $K_d$  distributions in function of environmental components (SS and DS) and conditions of liquid-solid exchange (adsorption, desorption, field)

Element	Component	Condition	GM L/kg	GSD	Min L/Kg	Max L/kg	5% L/Kg	95% L/Kg	Nd	Nr	K-S test	CI
Ag	DS	Field[0]	$5.25 \times 10^2$	n.a	n.a	n.a	n.a	n.a	1	1	n.r	0.14
Ag	SS	Adsorption	$8.30 \times 10^4$	2.28	$1.21 \times 10^4$	$1.58 \times 10^6$	$2.14 \times 10^4$	$3.22 \times 10^5$	81	7	OK	0.62
Ag	SS	Desorption	$4.10 \times 10^5$	1.73	$5.97 \times 10^4$	$9.48 \times 10^5$	$1.66 \times 10^5$	$1.01 \times 10^6$	41	2	OK	0.62
Ag	SS	Field[0]	$4.85 \times 10^5$	n.r	$1.08 \times 10^5$	$1.26 \times 10^6$	n.r	n.r	7	2	n.r	0.14
Al	SS	Field[0]	$4.62 \times 10^6$	n.r	$4.62 \times 10^6$	$2.75 \times 10^8$	n.r	n.r	2	1	n.r	0.14
Am	DS	Adsorption	$2.20 \times 10^5$	3.81	$2.70 \times 10^3$	$2.25 \times 10^6$	$2.44 \times 10^4$	$1.98 \times 10^6$	88	4	OK	0.41
Am	SS	Field[1]	$7.94 \times 10^4$	6.25	$1.10 \times 10^3$	$1.31 \times 10^6$	$3.90 \times 10^3$	$1.62 \times 10^6$	44	4	OK	0.41
As	DS	Field[0]	$4.26 \times 10^3$	3.47	$6.50 \times 10^1$	$2.93 \times 10^4$	$5.51 \times 10^2$	$3.29 \times 10^4$	35	7	OK	0.55
As	SS	Field[0]	$1.63 \times 10^4$	2.88	$9.32 \times 10^1$	$2.36 \times 10^5$	$2.86 \times 10^3$	$9.30 \times 10^4$	50	6	OK	0.62
B	SS	Field[1]	$1.41 \times 10^3$	2.56	$4.42 \times 10^2$	$6.20 \times 10^3$	$2.99 \times 10^2$	$6.62 \times 10^3$	21	1	OK	0.41
Ba	DS	Field[0]	$8.13 \times 10^3$	n.r	$8.13 \times 10^3$	$1.05 \times 10^4$	n.r	n.r	2	2	n.r	0.14
Ba	DS	Adsorption	$3.95 \times 10^2$	n.r	$4.50 \times 10^1$	$5.50 \times 10^2$	n.r	n.r	8	1	n.r	0.14
Ba	SS	Adsorption	$1.75 \times 10^3$	3.18	$7.20 \times 10^2$	$5.74 \times 10^3$	$2.61 \times 10^2$	$1.17 \times 10^4$	11	2	OK	0.62
Ba	SS	Field[2]	$7.95 \times 10^3$	2.75	$8.48 \times 10^2$	$7.84 \times 10^4$	$1.50 \times 10^3$	$4.21 \times 10^4$	70	6	OK	0.62
Be	SS	Adsorption	$1.60 \times 10^5$	n.r	$1.60 \times 10^5$	$3.60 \times 10^5$	n.r	n.r	2	1	n.r	0.14
Be	SS	Field[0]	$3.87 \times 10^4$	2.59	$2.20 \times 10^3$	$2.00 \times 10^5$	$8.06 \times 10^3$	$1.85 \times 10^5$	29	6	OK	0.48
Ca	DS	Field[0]	$1.38 \times 10^2$	n.r	$5.42 \times 10^1$	$1.47 \times 10^3$	n.r	n.r	3	2	n.r	0.14
Ca	SS	Field[1]	$1.35 \times 10^3$	1.44	$4.12 \times 10^2$	$5.50 \times 10^3$	$7.38 \times 10^2$	$2.46 \times 10^3$	23	3	OK	0.41
Cd	DS	Field[2]	$3.29 \times 10^2$	6.48	$7.69 \times 10^1$	$1.50 \times 10^4$	$1.52 \times 10^1$	$7.12 \times 10^3$	14	4	OK	0.55
Cd	SS	Field[2]	$6.78 \times 10^4$	2.07	$1.65 \times 10^3$	$2.40 \times 10^5$	$2.06 \times 10^4$	$2.24 \times 10^5$	33	6	OK	0.62
Ce	SS	Adsorption	$1.81 \times 10^5$	n.r	$5.30 \times 10^4$	$9.21 \times 10^5$	n.r	n.r	6	1	n.r	0.14
Ce	SS	Field[4]	$1.66 \times 10^5$	1.87	$7.25 \times 10^4$	$1.50 \times 10^6$	$5.91 \times 10^4$	$4.64 \times 10^5$	23	2	OK	0.41
Cm	DS	Adsorption	$1.64 \times 10^5$	6.81	$1.00 \times 10^4$	$2.25 \times 10^6$	$7.00 \times 10^3$	$3.86 \times 10^6$	29	1	OK	0.41
Cm	SS	Field[0]	$1.01 \times 10^5$	n.a	$5.25 \times 10^4$	$2.88 \times 10^5$	n.a	n.a	4	1	n.r	0.14
Co	DS	Adsorption	$1.59 \times 10^4$	10.40	$2.00 \times 10^1$	$5.43 \times 10^5$	$3.40 \times 10^2$	$7.48 \times 10^5$	300	8	NO	0.28
Co	DS	Desorption	$1.57 \times 10^4$	65.00	$6.76 \times 10^1$	$2.50 \times 10^6$	$1.63 \times 10^1$	$1.50 \times 10^7$	34	3	OK	0.72
Co	DS	Field[3]	$8.55 \times 10^1$	28.30	$2.00 \times 10^0$	$1.40 \times 10^5$	$3.50 \times 10^{-1}$	$2.09 \times 10^4$	20	4	OK	0.66
Co	SS	Adsorption	$8.76 \times 10^4$	13.8	$2.79 \times 10^2$	$1.13 \times 10^7$	$1.17 \times 10^3$	$6.56 \times 10^6$	234	16	OK	0.72
Co	SS	Desorption	$1.10 \times 10^6$	5.05	$1.20 \times 10^4$	$1.54 \times 10^7$	$7.71 \times 10^4$	$1.58 \times 10^7$	40	2	OK	0.79
Co	SS	Field[3]	$4.43 \times 10^4$	2.47	$3.70 \times 10^3$	$9.26 \times 10^5$	$1.00 \times 10^4$	$1.96 \times 10^5$	75	11	OK	0.62
Cr	DS	Field[3]	$1.76 \times 10^4$	14.30	$2.92 \times 10^2$	$1.29 \times 10^5$	$2.21 \times 10^2$	$1.41 \times 10^6$	25	4	OK	0.55
Cr	SS	Field[3]	$6.87 \times 10^4$	1.74	$1.23 \times 10^3$	$6.10 \times 10^5$	$2.76 \times 10^4$	$1.71 \times 10^5$	54	7	OK	0.55
Cs	DS	Adsorption	$4.97 \times 10^3$	9.74	$9.92 \times 10^0$	$6.06 \times 10^4$	$1.18 \times 10^2$	$2.10 \times 10^5$	366	10	NO	0.28
Cs	DS	Desorption	$1.35 \times 10^4$	5.67	$8.37 \times 10^2$	$2.10 \times 10^5$	$7.76 \times 10^2$	$2.33 \times 10^5$	55	3	NO	0.28
Cs	DS	Field[3]	$6.66 \times 10^3$	3.91	$7.25 \times 10^2$	$2.47 \times 10^5$	$7.06 \times 10^2$	$6.28 \times 10^4$	55	7	OK	0.66
Cs	SS	Adsorption	$1.71 \times 10^4$	2.47	$1.25 \times 10^3$	$1.37 \times 10^5$	$3.86 \times 10^3$	$7.58 \times 10^4$	203	15	OK	0.66
Cs	SS	Desorption	$3.30 \times 10^4$	2.50	$4.36 \times 10^3$	$1.38 \times 10^5$	$7.30 \times 10^3$	$1.49 \times 10^5$	64	4	OK	0.14
Cs	SS	Field[2]	$1.35 \times 10^5$	2.67	$2.34 \times 10^3$	$2.70 \times 10^6$	$2.64 \times 10^4$	$6.69 \times 10^5$	211	13	OK	0.79
Cu	DS	Field[0]	$7.28 \times 10^3$	21.40	$4.40 \times 10^0$	$2.94 \times 10^5$	$4.71 \times 10^1$	$1.13 \times 10^6$	62	15	NO	0.28
Cu	SS	Field[0]	$3.26 \times 10^4$	2.19	$1.05 \times 10^2$	$9.59 \times 10^6$	$8.96 \times 10^3$	$1.18 \times 10^5$	69	14	OK	0.48
Dy	DS	Field[3]	$5.80 \times 10^5$	2.53	$4.07 \times 10^4$	$3.66 \times 10^6$	$1.26 \times 10^5$	$2.66 \times 10^6$	26	1	OK	0.41
Er	DS	Field[3]	$4.85 \times 10^5$	2.24	$4.28 \times 10^4$	$3.24 \times 10^6$	$1.28 \times 10^5$	$1.83 \times 10^6$	26	1	OK	0.41
Eu	DS	Field[3]	$2.10 \times 10^5$	2.18	$2.69 \times 10^4$	$6.52 \times 10^5$	$5.81 \times 10^4$	$7.57 \times 10^5$	29	1	OK	0.41
Fe	DS	Field[0]	$3.28 \times 10^3$	69.10	$1.05 \times 10^1$	$5.00 \times 10^6$	$3.09 \times 10^0$	$3.47 \times 10^6$	32	9	OK	0.55
Fe	SS	Field[0]	$1.57 \times 10^5$	2.74	$2.41 \times 10^3$	$3.51 \times 10^6$	$2.99 \times 10^4$	$8.22 \times 10^5$	56	9	OK	0.55
Gd	DS	Field[3]	$4.26 \times 10^5$	3.16	$3.51 \times 10^4$	$4.35 \times 10^6$	$6.43 \times 10^4$	$2.82 \times 10^6$	29	1	OK	0.41
Hf	DS	Field[3]	$1.93 \times 10^6$	1.77	$3.77 \times 10^5$	$6.11 \times 10^6$	$7.56 \times 10^5$	$4.94 \times 10^6$	26	1	OK	0.41
Ho	DS	Field[3]	$4.25 \times 10^5$	1.97	$3.98 \times 10^4$	$1.16 \times 10^6$	$1.39 \times 10^5$	$1.30 \times 10^6$	26	1	OK	0.41
I	DS	Adsorption	$1.93 \times 10^1$	17.40	$7.47 \times 10^{-2}$	$4.00 \times 10^3$	$1.75 \times 10^{-1}$	$2.12 \times 10^3$	89	5	OK	0.66
I	SS	Adsorption	$3.62 \times 10^3$	4.17	$1.70 \times 10^2$	$1.05 \times 10^5$	$3.46 \times 10^2$	$3.78 \times 10^4$	71	5	OK	0.55
I	SS	Field[0]	$3.32 \times 10^3$	1.34	$7.88 \times 10^2$	$4.64 \times 10^3$	$2.06 \times 10^3$	$5.36 \times 10^3$	20	1	OK	0.41
K	SS	Field[1]	$1.93 \times 10^3$	2.14	$8.60 \times 10^2$	$1.01 \times 10^4$	$5.66 \times 10^2$	$6.95 \times 10^3$	21	1	OK	0.41
La	DS	Field[4]	$1.03 \times 10^6$	2.49	$3.72 \times 10^4$	$1.80 \times 10^7$	$2.31 \times 10^5$	$4.64 \times 10^6$	32	2	OK	0.41
La	SS	Field[4]	$1.36 \times 10^5$	1.69	$7.01 \times 10^4$	$4.09 \times 10^5$	$5.73 \times 10^4$	$3.21 \times 10^5$	21	1	OK	0.41
Li	DS	Field[3]	$7.60 \times 10^3$	2.08	$9.32 \times 10^1$	$5.01 \times 10^4$	$2.28 \times 10^3$	$2.54 \times 10^4$	32	1	OK	0.41
Mg	DS	Field[0]	$1.33 \times 10^2$	n.r	$6.25 \times 10^1$	$3.04 \times 10^2$	n.r	n.r	8	1	n.r	0.14
Mg	SS	Field[2]	$1.63 \times 10^3$	1.64	$8.45 \times 10^1$	$4.69 \times 10^3$	$7.26 \times 10^2$	$3.68 \times 10^3$	24	3	OK	0.41

Mn	DS	Adsorption	5.50×10 <sup>3</sup>	50.30	5.33×10 <sup>1</sup>	1.64×10 <sup>6</sup>	8.74×10 <sup>0</sup>	3.46×10 <sup>6</sup>	69	2	OK	0.83
Mn	DS	Desorption	5.94×10 <sup>3</sup>	n.r	1.87×10 <sup>3</sup>	1.64×10 <sup>6</sup>	n.r	n.r	6	1	n.r	0.14
Mn	DS	Field[1]	2.97×10 <sup>4</sup>	11.30	3.70×10 <sup>2</sup>	3.42×10 <sup>6</sup>	5.52×10 <sup>2</sup>	1.60×10 <sup>6</sup>	38	6	OK	0.83
Mn	SS	Adsorption	2.39×10 <sup>5</sup>	9.75	3.73×10 <sup>3</sup>	2.01×10 <sup>7</sup>	5.63×10 <sup>3</sup>	1.01×10 <sup>7</sup>	127	14	OK	0.79
Mn	SS	Desorption	1.33×10 <sup>6</sup>	6.33	2.70×10 <sup>4</sup>	1.00×10 <sup>7</sup>	6.38×10 <sup>4</sup>	2.76×10 <sup>7</sup>	40	2	OK	0.55
Mn	SS	Field[0]	7.21×10 <sup>4</sup>	3.15	1.63×10 <sup>3</sup>	2.20×10 <sup>8</sup>	1.09×10 <sup>4</sup>	4.76×10 <sup>5</sup>	75	13	OK	0.55
Mo	DS	Field[0]	7.27×10 <sup>1</sup>	n.r	4.16×10 <sup>1</sup>	2.69×10 <sup>2</sup>	n.r	n.r	3	2	n.r	0.14
Mo	SS	Field[1]	6.07×10 <sup>3</sup>	3.09	8.08×10 <sup>-1</sup>	7.11×10 <sup>6</sup>	9.48×10 <sup>2</sup>	3.89×10 <sup>4</sup>	29	2	OK	0.41
Na	SS	Field[3]	1.53×10 <sup>3</sup>	1.48	4.37×10 <sup>2</sup>	4.29×10 <sup>3</sup>	8.01×10 <sup>2</sup>	2.92×10 <sup>3</sup>	22	1	OK	0.41
Ni	DS	Field[3]	1.03×10 <sup>3</sup>	5.99	1.87×10 <sup>1</sup>	5.67×10 <sup>4</sup>	5.41×10 <sup>1</sup>	1.96×10 <sup>4</sup>	39	10	OK	0.55
Ni	SS	Field[3]	1.86×10 <sup>4</sup>	3.77	8.69×10 <sup>2</sup>	5.40×10 <sup>5</sup>	2.10×10 <sup>3</sup>	1.65×10 <sup>5</sup>	59	11	OK	0.62
Pb	DS	Field[3]	4.18×10 <sup>4</sup>	14.90	3.33×10 <sup>1</sup>	5.60×10 <sup>6</sup>	4.91×10 <sup>2</sup>	3.56×10 <sup>6</sup>	29	9	OK	0.62
Pb	SS	Field[2]	2.63×10 <sup>5</sup>	2.30	1.14×10 <sup>4</sup>	1.66×10 <sup>7</sup>	6.66×10 <sup>4</sup>	1.04×10 <sup>6</sup>	70	16	OK	0.62
Po	DS	Field[2]	1.02×10 <sup>5</sup>	5.35	2.21×10 <sup>4</sup>	6.10×10 <sup>6</sup>	6.45×10 <sup>3</sup>	1.61×10 <sup>6</sup>	10	2	OK	0.55
Po	SS	Field[1]	8.42×10 <sup>5</sup>	28.70	6.60×10 <sup>4</sup>	2.58×10 <sup>7</sup>	3.37×10 <sup>3</sup>	2.10×10 <sup>8</sup>	10	3	OK	0.55
Pr	SS	Field[4]	1.21×10 <sup>5</sup>	1.77	5.37×10 <sup>4</sup>	4.21×10 <sup>5</sup>	4.73×10 <sup>4</sup>	3.11×10 <sup>5</sup>	21	1	OK	0.41
Pu	DS	Adsorption	6.49×10 <sup>4</sup>	2.78	9.30×10 <sup>3</sup>	4.20×10 <sup>5</sup>	1.21×10 <sup>4</sup>	3.48×10 <sup>5</sup>	33	3	OK	0.55
Pu	DS	Desorption	2.96×10 <sup>5</sup>	2.05	3.07×10 <sup>4</sup>	1.25×10 <sup>7</sup>	9.07×10 <sup>4</sup>	9.65×10 <sup>5</sup>	41	4	OK	0.55
Pu	SS	Adsorption	6.04×10 <sup>4</sup>	n.r	6.00×10 <sup>3</sup>	3.00×10 <sup>6</sup>	n.r	n.r	4	1	n.r	0.14
Pu	SS	Field[1]	1.47×10 <sup>5</sup>	13.90	2.00×10 <sup>2</sup>	1.60×10 <sup>7</sup>	1.94×10 <sup>3</sup>	1.11×10 <sup>7</sup>	79	6	OK	0.41
Ra	DS	Adsorption	8.18×10 <sup>3</sup>	1.30	5.63×10 <sup>3</sup>	2.42×10 <sup>4</sup>	5.33×10 <sup>3</sup>	1.26×10 <sup>4</sup>	10	1	OK	0.41
Ra	DS	Field[3]	1.20×10 <sup>3</sup>	23.90	8.24×10 <sup>1</sup>	1.67×10 <sup>5</sup>	6.49×10 <sup>0</sup>	2.22×10 <sup>5</sup>	15	4	OK	0.48
Ra	SS	Adsorption	1.18×10 <sup>4</sup>	n.r	6.30×10 <sup>3</sup>	2.42×10 <sup>4</sup>	n.r	n.r	9	1	n.r	0.14
Ra	SS	Field[3]	5.21×10 <sup>3</sup>	2.76	1.13×10 <sup>2</sup>	1.73×10 <sup>5</sup>	9.79×10 <sup>2</sup>	2.77×10 <sup>4</sup>	48	3	OK	0.41
Rb	SS	Field[1]	7.33×10 <sup>3</sup>	1.92	2.12×10 <sup>3</sup>	2.38×10 <sup>4</sup>	2.50×10 <sup>3</sup>	2.15×10 <sup>4</sup>	21	1	OK	0.41
Ru	DS	Adsorption	5.28×10 <sup>4</sup>	1.39	3.34×10 <sup>4</sup>	7.90×10 <sup>4</sup>	3.09×10 <sup>4</sup>	9.03×10 <sup>4</sup>	36	1	OK	0.41
Ru	SS	Field[0]	2.73×10 <sup>4</sup>	1.67	4.00×10 <sup>2</sup>	5.39×10 <sup>4</sup>	1.17×10 <sup>4</sup>	6.36×10 <sup>4</sup>	38	2	OK	0.41
S	SS	Field[1]	1.33×10 <sup>3</sup>	1.55	7.25×10 <sup>2</sup>	7.06×10 <sup>3</sup>	6.44×10 <sup>2</sup>	2.73×10 <sup>3</sup>	21	1	OK	0.41
Sb	DS	Field[0]	1.20×10 <sup>4</sup>	n.r	1.09×10 <sup>4</sup>	1.94×10 <sup>4</sup>	n.r	n.r	3	1	n.r	0.14
Sb	SS	Adsorption	6.75×10 <sup>3</sup>	2.73	8.00×10 <sup>2</sup>	4.00×10 <sup>4</sup>	1.29×10 <sup>3</sup>	3.52×10 <sup>4</sup>	16	2	OK	0.41
Sb	SS	Field[3]	8.14×10 <sup>3</sup>	2.64	3.40×10 <sup>1</sup>	1.03×10 <sup>5</sup>	1.65×10 <sup>3</sup>	4.01×10 <sup>4</sup>	44	8	OK	0.41
Se	DS	Field[0]	7.08×10 <sup>3</sup>	n.a	n.a	n.a	n.a	n.a	1	1	n.r	0.14
Se	SS	Field[1]	1.54×10 <sup>4</sup>	2.19	5.41×10 <sup>3</sup>	6.65×10 <sup>4</sup>	4.24×10 <sup>3</sup>	5.61×10 <sup>4</sup>	22	1	OK	0.41
Si	SS	Field[1]	5.79×10 <sup>3</sup>	1.88	2.42×10 <sup>3</sup>	1.25×10 <sup>4</sup>	2.05×10 <sup>3</sup>	1.64×10 <sup>4</sup>	21	1	OK	0.41
Sn	SS	Field[0]	1.33×10 <sup>5</sup>	1.59	3.72×10 <sup>4</sup>	3.41×10 <sup>5</sup>	6.18×10 <sup>4</sup>	2.86×10 <sup>5</sup>	21	1	OK	0.41
Sr	DS	Adsorption	5.01×10 <sup>1</sup>	3.21	2.84×10 <sup>0</sup>	1.34×10 <sup>3</sup>	7.34×10 <sup>0</sup>	3.42×10 <sup>2</sup>	126	5	NO	0.28
Sr	DS	Desorption	4.81×10 <sup>2</sup>	2.23	3.46×10 <sup>1</sup>	2.06×10 <sup>3</sup>	1.29×10 <sup>2</sup>	1.80×10 <sup>3</sup>	34	3	OK	0.41
Sr	DS	Field[0]	1.38×10 <sup>2</sup>	n.a	6.00×10 <sup>0</sup>	3.45×10 <sup>3</sup>	n.a	n.a	8	4	n.r	0.14
Sr	SS	Adsorption	1.42×10 <sup>3</sup>	1.34	4.80×10 <sup>2</sup>	2.48×10 <sup>3</sup>	8.76×10 <sup>2</sup>	2.30×10 <sup>3</sup>	30	2	OK	0.66
Sr	SS	Field[2]	2.96×10 <sup>3</sup>	3.79	1.11×10 <sup>2</sup>	1.99×10 <sup>4</sup>	3.31×10 <sup>2</sup>	2.65×10 <sup>4</sup>	39	5	OK	0.66
Th	DS	Adsorption	1.56×10 <sup>5</sup>	47.80	1.15×10 <sup>2</sup>	2.75×10 <sup>6</sup>	2.69×10 <sup>2</sup>	9.04×10 <sup>7</sup>	12	2	OK	0.41
Th	DS	Field[0]	7.40×10 <sup>2</sup>	n.a	3.60×10 <sup>2</sup>	4.72×10 <sup>5</sup>	n.a	n.a	9	3	n.r	0.14
Th	SS	Field[0]	1.52×10 <sup>5</sup>	2.90	1.13×10 <sup>4</sup>	1.60×10 <sup>6</sup>	2.64×10 <sup>4</sup>	8.76×10 <sup>5</sup>	41	4	OK	0.41
Ti	DS	Field[0]	4.07×10 <sup>4</sup>	n.a	n.a	n.a	n.a	n.a	1	1	n.r	0.14
Ti	SS	Field[2]	1.05×10 <sup>5</sup>	1.35	2.41×10 <sup>4</sup>	1.58×10 <sup>5</sup>	6.42×10 <sup>4</sup>	1.71×10 <sup>5</sup>	21	1	OK	0.41
U	DS	Field[2]	3.50×10 <sup>3</sup>	40.10	9.10×10 <sup>1</sup>	8.04×10 <sup>4</sup>	8.07×10 <sup>0</sup>	1.51×10 <sup>6</sup>	14	5	OK	0.41
U	SS	Field[1]	1.19×10 <sup>4</sup>	5.63	3.05×10 <sup>2</sup>	1.27×10 <sup>5</sup>	6.94×10 <sup>2</sup>	2.04×10 <sup>5</sup>	38	6	OK	0.41
V	DS	Field[0]	3.71×10 <sup>4</sup>	n.a	n.a	n.a	n.a	n.a	1	1	n.r	0.14
V	SS	Field[2]	4.29×10 <sup>4</sup>	1.40	1.19×10 <sup>4</sup>	8.46×10 <sup>4</sup>	2.47×10 <sup>4</sup>	7.44×10 <sup>4</sup>	21	1	OK	0.41
Zn	DS	Field[2]	1.49×10 <sup>2</sup>	32.40	2.11×10 <sup>0</sup>	1.71×10 <sup>4</sup>	4.89×10 <sup>-1</sup>	4.53×10 <sup>4</sup>	31	7	OK	0.55
Zn	SS	Field[2]	7.20×10 <sup>4</sup>	2.68	3.00×10 <sup>3</sup>	3.32×10 <sup>7</sup>	1.43×10 <sup>4</sup>	3.64×10 <sup>5</sup>	50	11	OK	0.62

(\*) indicates median values. No (\*) corresponds to geometric means.

Nd = number of data

Nr = number of references

n.a = not available

n.r = not relevant

Field[X]: Representativeness of  $K_d$  datasets for field conditions (see 4.1 for SS and 4.2 for DS):

Field[0]: no information; Field[1]: relevant for anthropic releases; Field[2]: relevant for anthropic releases with a risk of overestimation; Field[3] and Field[4]: relevant for environmental conditions.

**Table 3:** Parameters  $a$  and  $b$ , determination coefficients  $R^2$  and p-value of parameter  $b$  of the Equation 3 - (\*) indicates the elements with p-value  $> 0.05$

Element	$a$	$b$ (p-value)	$R^2$	Element	$a$	$b$ (p-value)	$R^2$
<b>Am</b>	$6.09 \times 10^5$	-0.839 ( $1.00 \times 10^{-6}$ )	0.44	<b>Ni</b>	$5.21 \times 10^4$	-0.462 ( $2.30 \times 10^{-3}$ )	0.18
<b>As</b> (*)	$4.51 \times 10^4$	-0.254 ( $8.00 \times 10^{-2}$ )	0.07	<b>Pb</b>	$2.00 \times 10^6$	-0.610 ( $3.30 \times 10^{-13}$ )	0.60
<b>B</b>	$2.54 \times 10^4$	-1.368 ( $3.30 \times 10^{-7}$ )	0.75	<b>Po</b>	$1.00 \times 10^6$	-1.290 ( $5.00 \times 10^{-7}$ )	0.97
<b>Ba</b>	$3.37 \times 10^4$	-0.515 ( $1.50 \times 10^{-2}$ )	0.54	<b>Pr</b>	$4.00 \times 10^4$	0.5694 ( $1.70 \times 10^{-2}$ )	0.26
<b>Be</b> (*)	$4.49 \times 10^4$	-0.066 ( $4.30 \times 10^{-1}$ )	0.02	<b>Pu</b>	$7.15 \times 10^5$	-0.990 ( $1.25 \times 10^{-6}$ )	0.40
<b>Ca</b>	$8.01 \times 10^3$	-0.838 ( $4.40 \times 10^{-7}$ )	0.73	<b>Ra</b>	$2.25 \times 10^4$	-0.238 ( $2.00 \times 10^{-3}$ )	0.19
<b>Cd</b>	$2.35 \times 10^5$	-0.531 ( $9.35 \times 10^{-8}$ )	0.67	<b>Rb</b>	$7.48 \times 10^4$	-1.104 ( $6.25 \times 10^{-9}$ )	0.84
<b>Ce</b>	$7.85 \times 10^4$	0.320 ( $1.60 \times 10^{-3}$ )	0.34	<b>S</b>	$8.03 \times 10^3$	-0.833 ( $9.70 \times 10^{-6}$ )	0.65
<b>Co</b>	$6.97 \times 10^4$	-0.160 ( $1.20 \times 10^{-2}$ )	0.09	<b>Sb</b>	$2.70 \times 10^4$	-0.374 ( $1.00 \times 10^{-3}$ )	0.25
<b>Cr</b>	$1.18 \times 10^5$	-0.227 ( $1.70 \times 10^{-2}$ )	0.11	<b>Se</b>	$1.52 \times 10^5$	-1.096 ( $8.30 \times 10^{-6}$ )	0.66
<b>Cs</b>	$1.80 \times 10^5$	-0.493 ( $4.10 \times 10^{-6}$ )	0.26	<b>Si</b>	$3.20 \times 10^4$	-0.813 ( $1.00 \times 10^{-4}$ )	0.56
<b>Cu</b> (*)	$6.09 \times 10^4$	-0.152 ( $2.00 \times 10^{-1}$ )	0.03	<b>Sn</b> (*)	$3.18 \times 10^5$	-0.428 ( $6.20 \times 10^{-2}$ )	0.17
<b>Fe</b> (*)	$2.92 \times 10^5$	-0.136 ( $2.00 \times 10^{-1}$ )	0.04	<b>Sr</b>	$1.10 \times 10^4$	-0.587 ( $6.00 \times 10^{-5}$ )	0.36
<b>K</b>	$3.60 \times 10^4$	-1.324 ( $2.33 \times 10^{-7}$ )	0.76	<b>Th</b> (*)	$1.41 \times 10^5$	0.504 ( $2.11 \times 10^{-1}$ )	0.13
<b>La</b>	$5.06 \times 10^4$	0.5133 ( $2.00 \times 10^{-2}$ )	0.25	<b>Ti</b>	$2.94 \times 10^5$	-0.526 ( $3.20 \times 10^{-3}$ )	0.37
<b>Mg</b>	$7.08 \times 10^3$	-0.654 ( $1.20 \times 10^{-3}$ )	0.43	<b>U</b>	$9.72 \times 10^4$	-0.783 ( $5.00 \times 10^{-7}$ )	0.52
<b>Mn</b> (*)	$1.43 \times 10^5$	-0.150 ( $2.22 \times 10^{-1}$ )	0.02	<b>V</b>	$1.44 \times 10^5$	-0.625 ( $6.00 \times 10^{-3}$ )	0.34
<b>Mo</b>	$1.14 \times 10^5$	-1.228 ( $1.71 \times 10^{-6}$ )	0.59	<b>Zn</b>	$3.91 \times 10^5$	-0.575 ( $1.30 \times 10^{-4}$ )	0.29
<b>Na</b>	$3.49 \times 10^3$	-0.360 ( $3.30 \times 10^{-2}$ )	0.22				

## List of Figures

**Figure 1:** Ratio between the element concentration in superficial dried deposited sediments ( $C_{DS}$ ) with that in the water column ( $C_{wc}$ ) for a pulse input of a pollutant element

**Figure 2:** Distribution of the  $K_d$  datasets of the 49 listed elements for the six combinations between components and conditions

**Figure 3:**  $CI$  values for  $K_d$  distributions under field conditions

**Figure 4:**  $K_d$  of  $SS$  in the field in function of  $M/V$  for Cs, Am, Pu and Sr

**Figure 5:** Determination coefficients of Equation 3 in function of  $b$

**Figure 6:**  $K_d$  distributions for  $SS$  and  $DS$  in the case of adsorption (a), desorption (b) and field conditions (c) (the point corresponds to the  $GM$  and the upper and lower error bars correspond to 5 and 95 percentiles respectively)

**Figure 7:** Ratio of  $GSD$  values between  $SS$  and  $DS$  in the case of adsorption (a), desorption (b) and field conditions (c)

**Figure 8:**  $GM(K_d)$  for  $DS$  in the field divided by  $a \cdot SS^b$  for  $SS = 650$  g/L

**Figure 9:**  $K_d$  distributions of  $DS$  (a) and  $SS$  (b) as a function of exchange conditions (points correspond to  $GM$  and high and low levels correspond respectively to 5 and 95 percentiles)

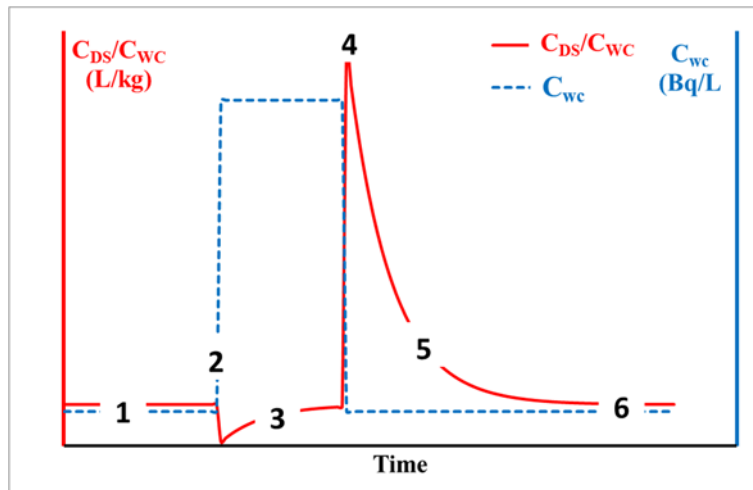


**Figure 4:** Ratio between the element concentration in superficial dried deposited sediments ( $C_{DS}$ ) with that in the water column ( $C_{wc}$ ) for a pulse input of a pollutant element

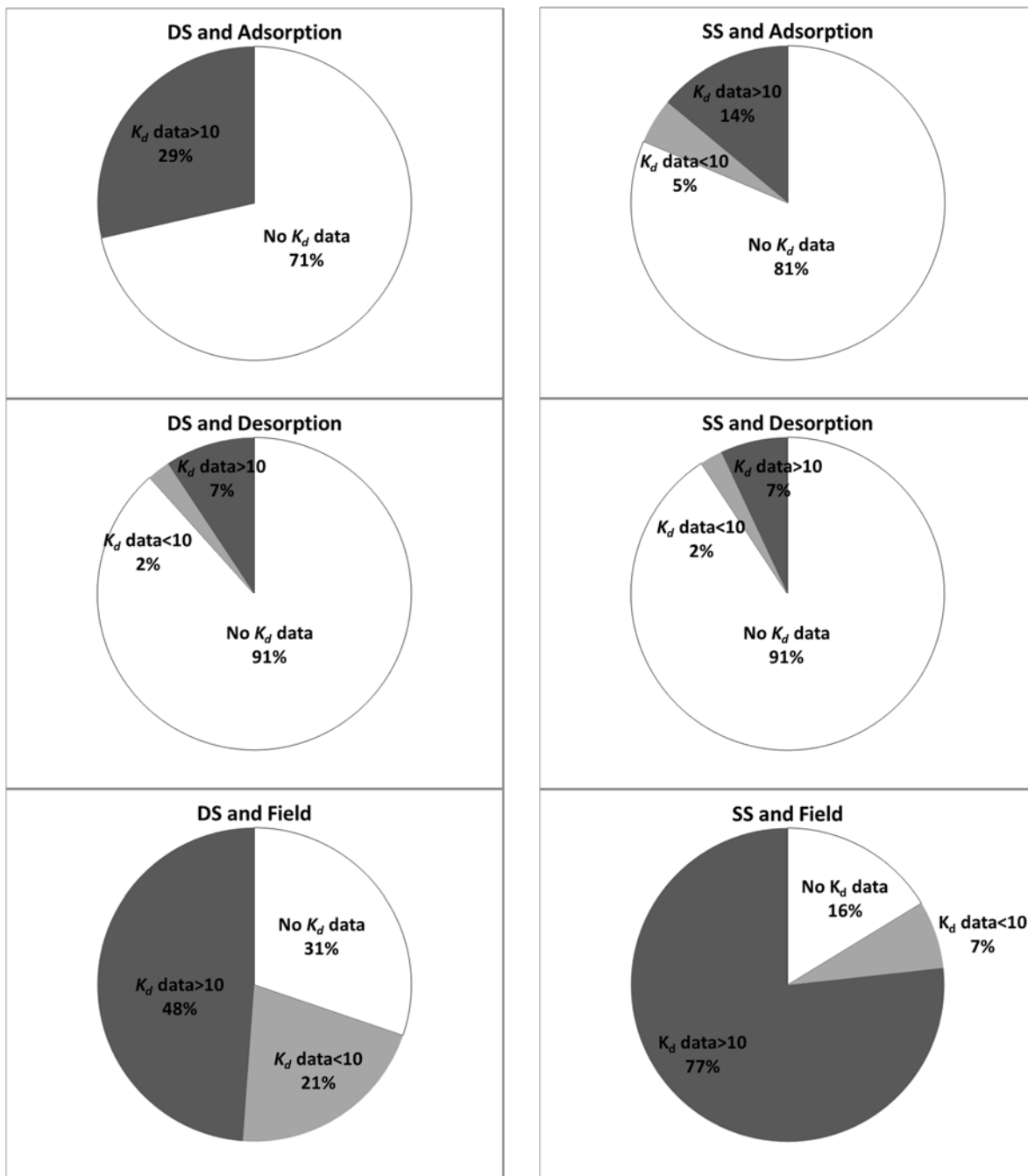


**Figure 5:** Distribution of the  $K_d$  datasets of the 49 listed elements for the six combinations between components and conditions

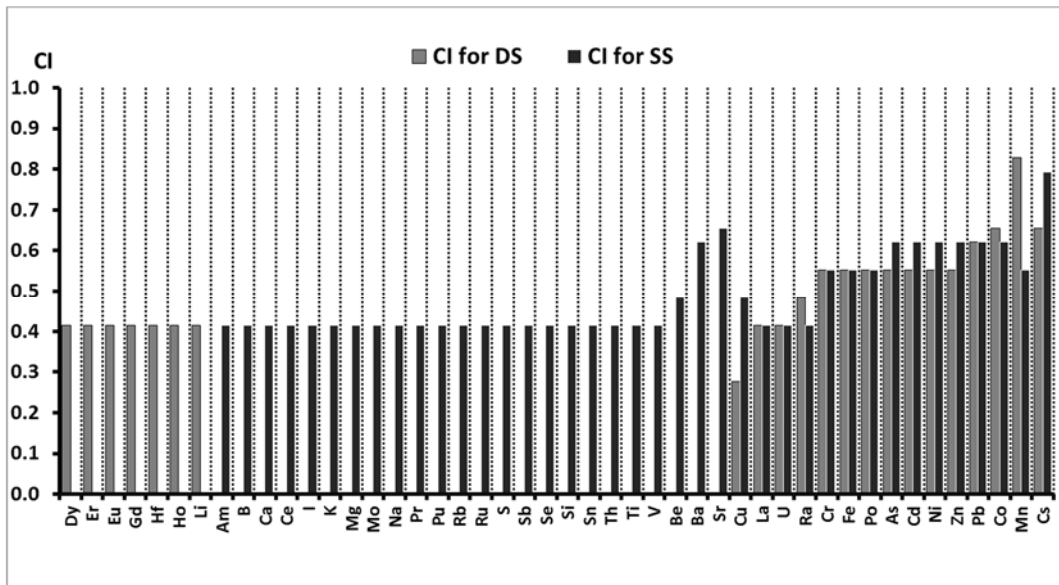


**Figure 6:**  $CI$  values for  $K_d$  distributions under field conditions

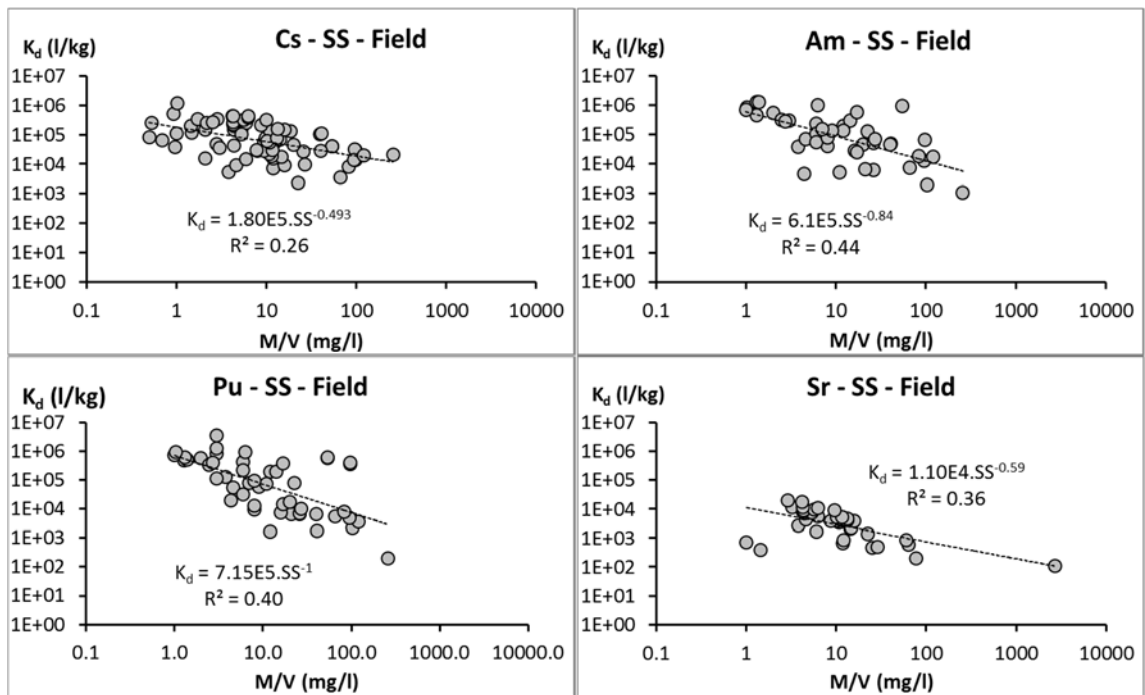


**Figure 4:**  $K_d$  of SS in the field in function of  $M/V$  for Cs, Am, Pu and Sr

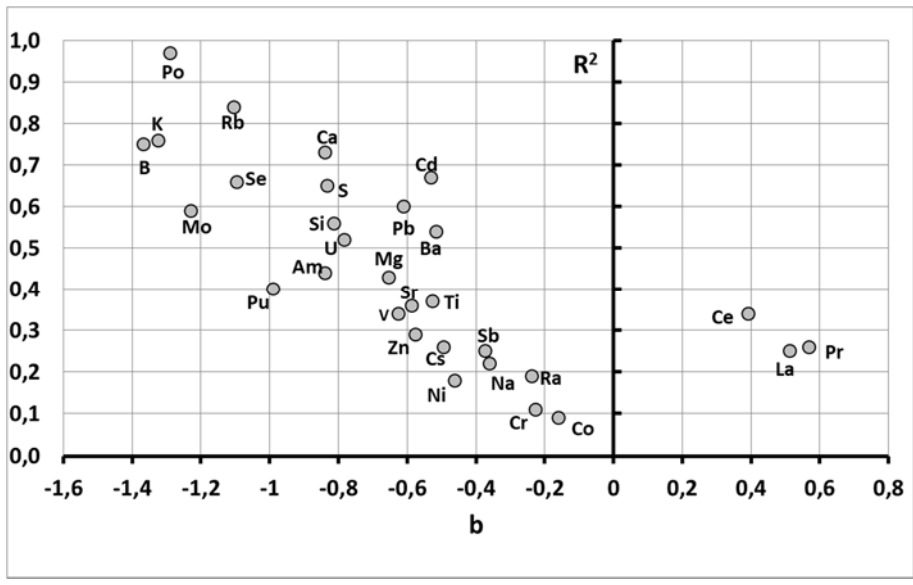


**Figure 5:** Determination coefficients of Equation 3 in function of  $b$

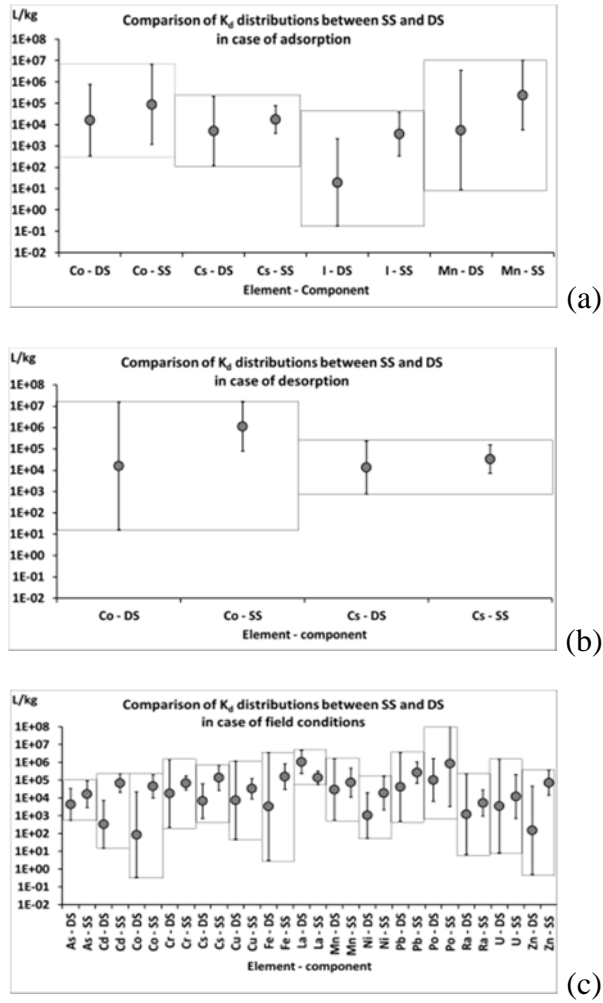


**Figure 6:**  $K_d$  distributions for SS and DS in the case of adsorption (a), desorption (b) and field conditions (c) (the point corresponds to the  $GM$  and the upper and lower error bars correspond to 5 and 95 percentiles respectively)

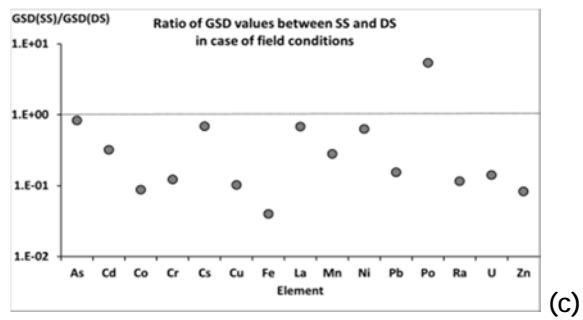
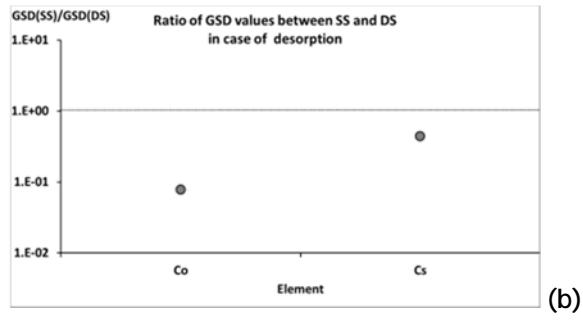
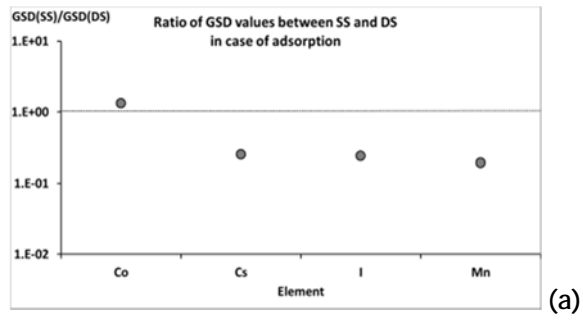


**Figure 7:** Ratio of *GSD* values between *SS* and *DS* in the case of adsorption (a), desorption (b) and field conditions (c)

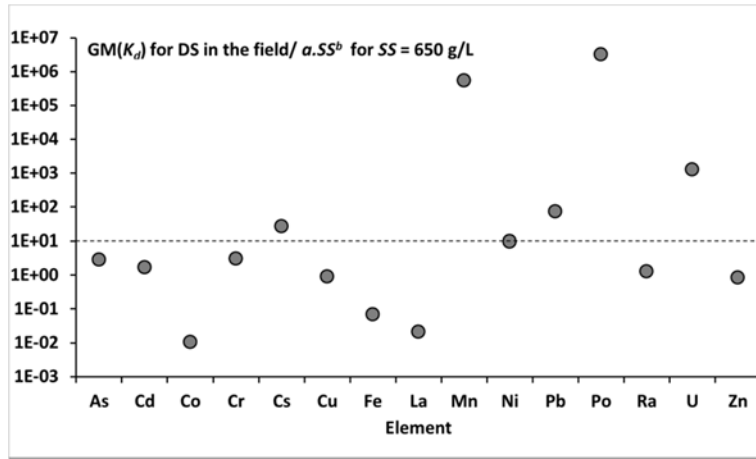


**Figure 8:**  $GM(K_d)$  for  $DS$  in the field divided by  $a.SS^b$  for  $SS = 650$  g/L

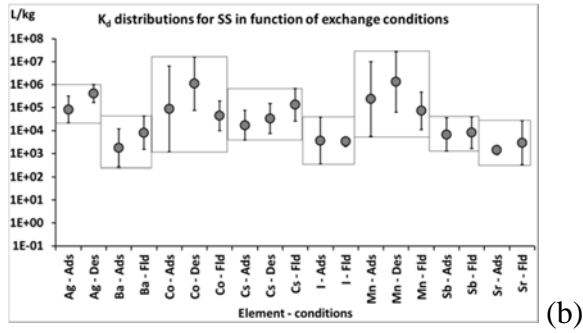
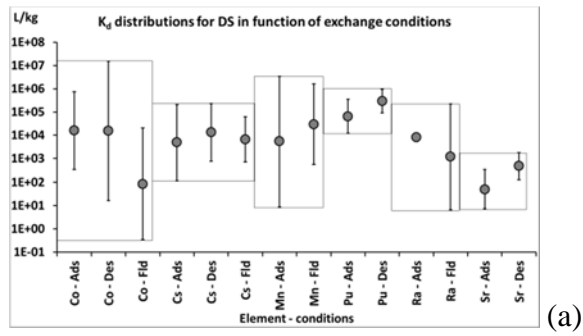


**Figure 9:**  $K_d$  distributions of *DS* (a) and *SS* (b) as a function of exchange conditions (points correspond to *GM* and high and low levels correspond respectively to 5 and 95 percentiles)